UNIVERSITY OF DURHAM

DEPARTMENT OF MATHEMATICAL SCIENCES

Mathematical Modelling of the Violin

Author:
Oliver M. Brown

Supervisor:
Prof. Bernard Piette

April 29, 2022

Plagarism Declaration

This piece of work is a result of my own work except where it forms an assessment based on group project work. In the case of a group project, the work has been prepared in collaboration with other members of the group. Material from the work of others not involved in the project has been acknowledged and quotations and paraphrases suitably indicated.

Abstract

This project studies a series of models for the vibrations of different parts of a violin. The theory of elasticity is used to calculate the elastic energies of materials and from this several differential equations are derived to model the vibrations of the strings, and the body, of the violin. The wave equation is derived and solved to describe the motion of the bowed string. A fourth order differential equation, the Kirchoff-Love equation, is derived to model the vibrations of a thin elastic plate. The solutions to this fourth order PDE are compared to experimental results and the equation is then solved numerically to model the vibrations in a violin-shaped body, driven by vibrations through the sound post.

Acknowledgements

Contents

Chapter 1

Introduction

"I know that the most joy in my life has come to me from my violin."

- Albert Einstein[I]

1.1 The violin

The violin is a fascinating and beautiful instrument. The modern violin was first developed in northern Italy in the early 16th century [1], and the art of violin making reached its height during the 17th century in Cremona with the work of the famed violin-makers Nicolo Amati and Antonio Stradivari. Their superb skill in violin-making came not from any scientific knowledge of the acoustics of stringed instruments, but instead from a wealth of practical experience. The development of the violin was, in fact, blind to the remarkable mathematics and physics that lies behind the study of music. In the centuries since the instrument was first developed, the effort to better understand how the violin produces its enchanting sound has driven huge progress in our scientific understanding of acoustics and materials.

To produce a sound from a violin, a musician draws the bow across one of the violin's four strings, between the bridge and the fingerboard and perpendicular to the string. The violinist places the fingers of the hand which supports the instrument on the violin's fingerboard in order to change the length of the vibrating string, thereby changing the note played when the string is bowed (figure 1.1). These vibrations propagate into the body of the violin through a wooden structure called the bridge, on top of which the four strings rest.

Figure 1.1: The famed violinist Yehudi Menuhin. He played the Soil Stradivarius, considered one of the finest violins made by Antonio Stradivari.[II]

[I]https://www.classicfm.com/discover-music/latest/quotes-about-classical-music/albert-einstein/
[II]https://www.warnerclassics.com/artist/yehudi-menuhin
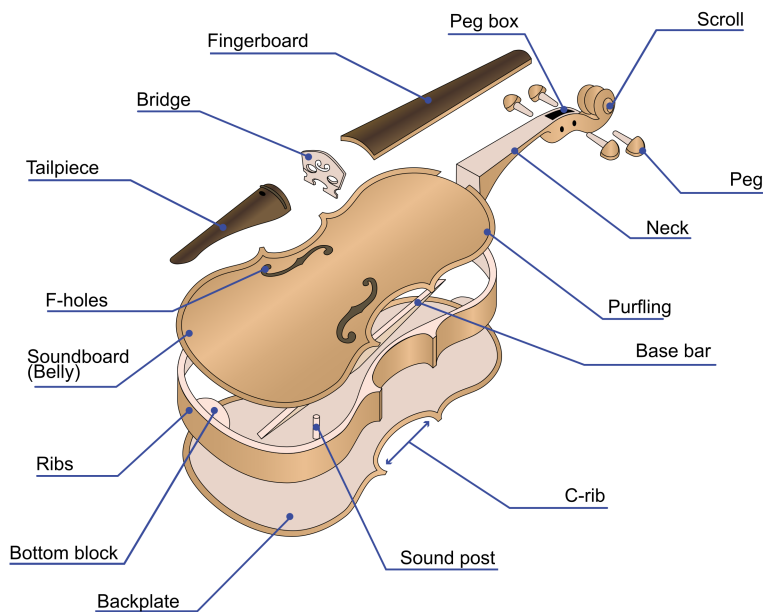
Figure 1.2: The structure of the violin.[III]

The vibrations produced by the strings are then transmitted down through the bridge to a structure called the sound post. The sound post is a wooden rod that is connected to the base plate of the violin, and supports the bridge (figures 1.2 and 1.3). As the vibrations propagate through the sound post, the vibration of the sound post induces the back plate to vibrate at a particular mode of resonance. The soundboard (front plate) of the violin contains two f-shaped holes, unsurprisingly known as f-holes, which allows sound waves transmitted through air to pass out from the interior of the violin. This enables the violin body to act as a sound box, coupling the vibrations of the strings to the air in order to amplify the sound of the strings.
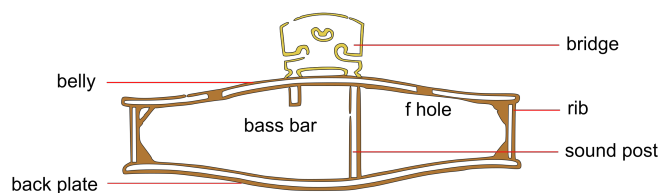
Figure 1.3: The interior of the violin.[III]

The intricate shape of the violin was developed in order to produce a thin wooden plate for which the normal modes can be produced by inducing resonance in the plate at the precise frequencies of *musical notes*. If the resonant frequencies of the back plate did not correspond to the frequencies of musical notes, then the violin would be essentially useless as a musical instrument. As a result, when we study the modes of resonance of the violin's back plate, we need to take account for both the properties of the wood and its thickness, as well as the shape of the plate.

[III]Amitchell125, Wikimedia Commons

1.2 Helmoltz motion

In the 19th century, German physicist Hermann von Helmholtz carried out experiments to study the waveforms produced on the strings of bowed violins [2]. He discovered that as the string is bowed, the displacement at any particular point on the string with respect to time follows a zig-zagged pattern (figure 1.4) [3]. This pattern is interpreted as a result of the string alternating between sticking to, and slipping against, the bow. At every point, the string will either be moving with the bow at a constant speed, or slipping back against the bow at a different constant speed.
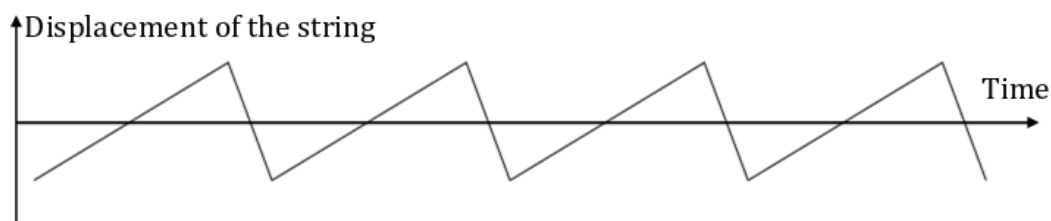
Figure 1.4: The displacement of the string at particular position with respect to time. The displacement curve shows a constant speed of displacement with the bow and a different speed of slip-back against the bow [4].

Physically, what this is describing is the motion of a string which oscillates in a triangular shape, with the apex of the triangle prescribed by a parabola (figure 1.5). This shape allows for each point on the string to be either moving with the bow, or slipping back against the bow.
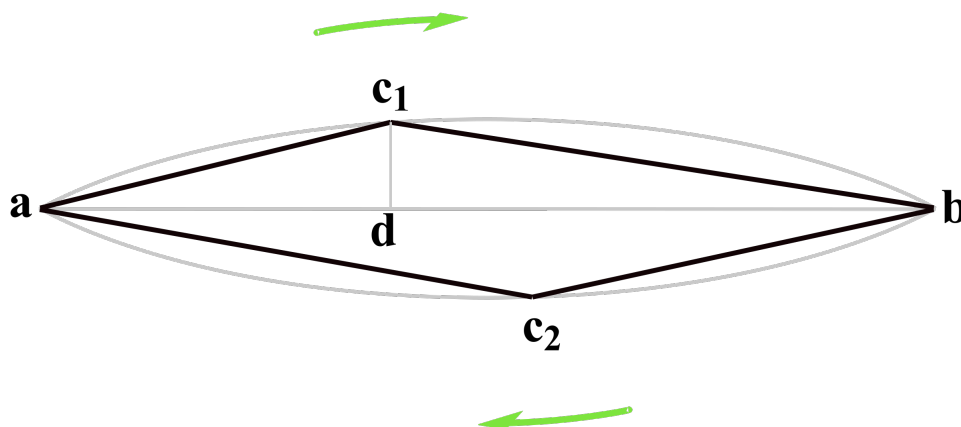
Figure 1.5: The triangular shape discovered by Helmholtz. The apex of the triangle moves from a to b, and back again.[III]

This triangular shaped wave can be described mathematically as a periodic function defined only on $x \in [0, L]$, where L is the length of the string. As any periodic function can be decomposed using Fourier analysis into a superposition of standing waves of different frequencies, we can deduce that the triangular Helmholtz waveform on the string actually contains a spectrum of frequencies, not just the fundamental frequency of that string. These frequencies are then transmitted through the bridge into the body of the violin.

1.3 Chladni patterns

The first recorded discovery of the vibrational modes of a thin plate comes from Galileo [5]. He describes in *Two New Sciences* that

> *"As I was scraping a brass plate with a sharp iron chisel in order to remove some spots from it and was running the chisel rather rapidly over it, I once or twice, during many strokes, heard the plate emit a rather strong and clear whistling sound; on looking at the plate more carefully, I noticed a long row of fine streaks parallel and equidistant from one another."*

Following this, Robert Hooke conducted experiments in July 1680 to observe the nodal patterns associated with the vibrations of glass plates [6]. Hooke drew a violin bow along the edge of a plate with its surface covered in flour and saw the nodal patterns that emerged. A more detailed study was conducted in 1787 by the German mathematician Ernst Chladni (figure 1.6) [7]. Chladni's technique similarly involved drawing a bow over a piece of metal whose surface was thinly covered with sand. The plate was bowed so that the plate resonated, at which point the vibrations cause the sand to move and collect along the lines where the surface is still, outlining the nodal lines (figure 1.7). In honour of his work, the patterns formed by these lines are now known as *Chladni patterns*.

Figure 1.6: Ernst Chladni, 1756-1827. As well as his foundational work in acoustics, he is also known for his pioneering studies into the origins of meteorites.[IV]
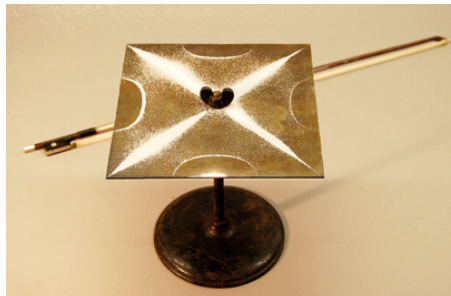
Figure 1.7: Chladni pattern of a mode of vibration found for a square brass plate.[V]

When a flat plate vibrates in a particular mode of resonance, the surface of the plate is split into regions oscillating in opposing directions, bounded by nodal lines which remain stationary. When a light powder is distributed across the surface of the vibrating plate, the powder will be brushed away from the oscillating regions, coming to rest along the nodal lines for that particular mode of resonance. As these patterns provide a way to not only visualize the normal modes of vibrations for a thin elastic plate, but also to check which resonant frequencies these modes appear at, the Chladni patterns are of huge importance in acoustics.

[IV]Lithograph by Ludwig Albert von Montmorillon, circa 1825, Deutschen Staatsbibliothek, Berlin.

[V]https://americanhistory.si.edu/science/chladni.htm
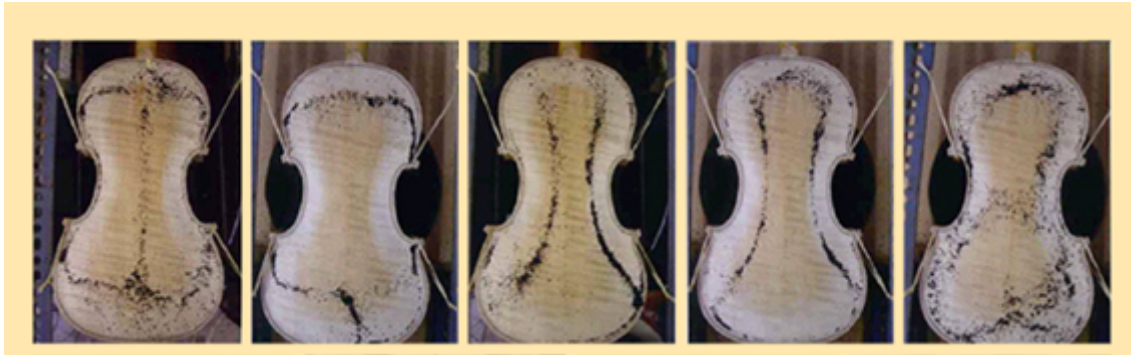
Figure 1.8: Chladni patterns for modes of resonance for a violin back plate [8].

Chladni's method is now a vital technique in the craft of violin-making, as explained by violin maker Benning Violins[VI]: once a violin-maker has carved out the back plate for their violin, they must then test whether the plate has been manufactured to precisely the right shape and thickness in order to resonate at the frequencies of musical notes. The violin-maker will plate the back plate atop a speaker which produces sound waves at the required musical frequencies, and will cover the plate in tea leaves. The tea leaves should form a characteristic pattern for the modes of resonance for each frequency. When using the Chladni technique, a symmetrical violin plate will form symmetrical Chladni Patterns (figure 1.8). The violin-maker can then use the patterns as a guide for adjusting the symmetry of the plate and finding acoustical balance, essentially tuning the resonances of the instrument (figure 1.9). Adjustments are then made to the shape of the violin plate or to the thickness by scraping the surface of the violin plate [9].
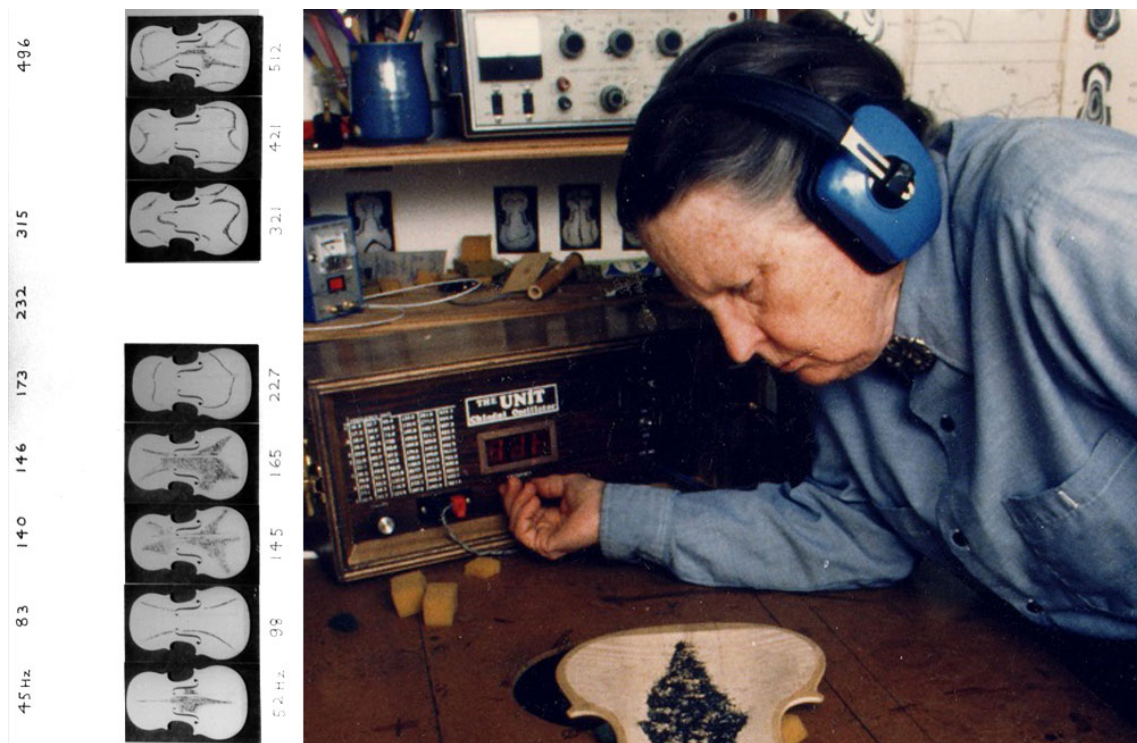
Figure 1.9: A violin-maker studying the Chladni patterns for a back plate that has been manufactured.[VI]

1.4 Sophie Germain's prize

In 1808, Chladni visited the Paris Academy of Sciences and demonstrated the vibration patterns to an audience that included not only the greatest French scientists of the time, but also Emperor Napoleon [10]. Amazed by Chladni's method of visualizing two-dimensional harmonic motion, Napoleon set a prize known as the *"Prix Extraordinaire"* for the best mathematical explanation of this phenomenon.

Sophie Germain (figure 1.10) quickly set about working on this problem. Solving it would require signicant development of the theory of elastic surfaces, which was not well-established at the time. After several unsuccessful attempts, and with some assistance from Joseph-Louis Lagrange, she submitted in January 1816 her paper "Recherches sur la théorie des surfaces élastiques" and became the first woman to win a prize from the Paris Academy of Sciences [11]. In this paper she derived the correct differential equation to describe the normal modes of an elastic plate, however as her boundary conditions were incorrect, her theory did not accurately predict experimental results.

Figure 1.10: Sophie Germain, 1776-1831. Her attempts to prove Fermat's Last Theorem also led to developments in number theory.[VII]

The differential equation which she derived was

$$N^2\left(\frac{\partial^4 v}{\partial x^4} + 2\frac{\partial^4 v}{\partial x^2 \partial y^2} + \frac{\partial^4 v}{\partial y^4}\right) + \frac{\partial^2 v}{\partial t^2} = 0, \tag{1.1}$$

where N^2 is a constant [12]. This equation (without the time derivative, which can be removed by separation of variables) is sometimes known as the Germain-Lagrange equation [13].
Using the work of Gustav Kirchoff as a basis, A. E. H. Love was able to derive a more general form of this equation,

$$-q(x,y,t) - 2\rho h\frac{\partial^2 v}{\partial t^2} = D\left(\frac{\partial^4 v}{\partial x^4} + 2\frac{\partial^4 v}{\partial x^2 \partial y^2} + \frac{\partial^4 v}{\partial y^4}\right). \tag{1.2}$$

We will derive this equation, and show that it can be used to model the modes of vibration of a thin elastic plate. This is the equation that should predict the Chladni patterns for a thin plate.

Chapter 2

The Theory of Elasticity

In order to model the vibrations in the components of the violin body, we must find some way to derive differential equations to describe how an elastic vibration will propagate through the material.

To do this, we study the internal motion of a continuous medium through *stresses* (internal forces) and *strains* (internal displacements) in the theory of *linear elasticity*. Finding an appropriate relationship between stresses and strains in an isotropic material allows us to derive equations of motion for elastic waves in the medium. Furthermore, we can find expressions for the general kinetic and potential energies of elastic deformations which will allow us to derive differential equations for elastic vibrations in different structures along with relevant boundary conditions.

This chapter loosely follows David J. Raymond's *"Introduction to Continuum Mechanics"* [14], and L. D. Landau and E. M. Lifschitz's *"Theory of Elasticity"* [15].

2.1 The stress tensor

The internal forces of a continuous material cannot be described by a single three-dimensional vector. If we were to use a single vector to describe the forces on each infinitesimally small section of the material, then we could only describe translations of each material point, and not rotations, stretching, or shear forces. Instead, we use three separate vectors arranged into a 3×3 matrix called the *stress tensor*.

Consider two regions of a material, with a force $\mathbf{T}$ applied between them. The force applied by region 1 on region 2 is composed of a "pushing" force normal to the surface, and a "shear" force causing the material in each region to slide parallel to the surface. This force is called the *traction* of region 1 on region 2 as is represented by a *traction vector*, $\mathbf{T}$ (figure 2.1).

At any given point in a material, it is possible to find three different traction vectors by finding the tractions along three different orthogonal surfaces. For example, if we pick a point in the material and draw a surface normal to the x direction (i.e. in the y-z plane), then we can define the traction $\mathbf{T_x}$ to be the traction force on this surface (figure 2.2).

Figure 2.1: The traction force between two regions in a solid material

Region 1

Traction force

Region 2
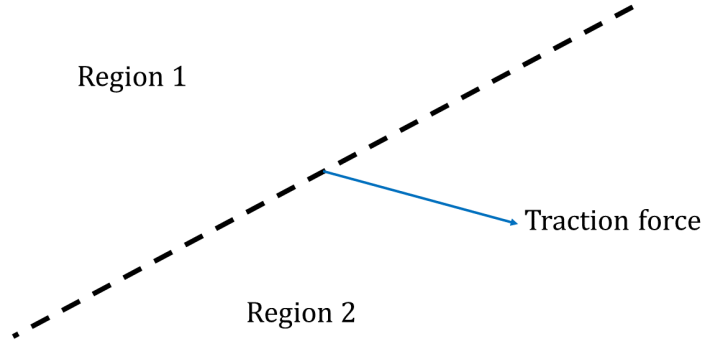
Figure 2.2: The traction forces at a point defined on three mutually orthogonal surfaces
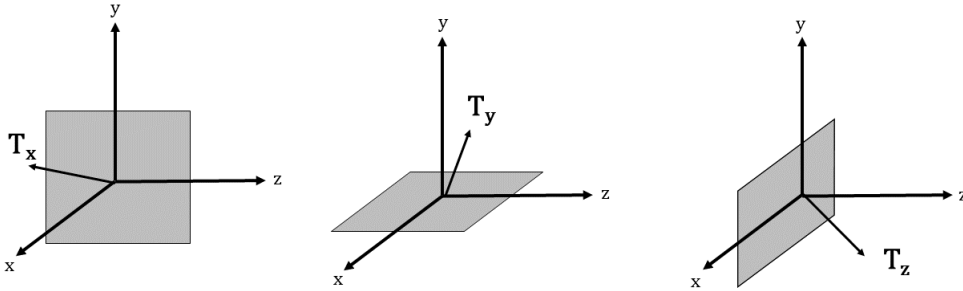
We can place these three traction vectors into a matrix called the Cauchy stress tensor.

Definition 2.1.1 (Cauchy Stress Tensor). At every point in some body, the *Cauchy stress tensor* is defined to be

$$\sigma = \begin{bmatrix} \boldsymbol{T_x}^t \\ \boldsymbol{T_y}^t \\ \boldsymbol{T_z}^t \end{bmatrix} = \begin{bmatrix} T_{xx} & T_{xy} & T_{xz} \\ T_{yx} & T_{yy} & T_{yz} \\ T_{zx} & T_{zy} & T_{zz} \end{bmatrix}, \tag{2.1}$$

where $\mathbf{T_x}$, $\mathbf{T_y}$ and $\mathbf{T_z}$ are defined to be the tractions on planes normal to the x, y and z axes respectively. Each traction vector here has been decomposed into x, y and z components by

$$\boldsymbol{T_x} = T_{xx}\boldsymbol{e_x} + T_{xy}\boldsymbol{e_y} + T_{xz}\boldsymbol{e_z}, \tag{2.2}$$

and similar for $\mathbf{T_y}$ and $\mathbf{T_z}$.

To find the traction $\mathbf{T_n}$ on an arbitrary surface normal to a vector $\hat{\mathbf{n}}$, we calculate

$$\boldsymbol{T_n} = \sigma \cdot \hat{\boldsymbol{n}}. \tag{2.3}$$

2.2   Equations of motion

To derive the equation of motion for material elements in a solid, we consider the forces on a small cube within the material of side length l. The force on the side of the cube located at position $x = x'$ is given by the traction $\boldsymbol{T}(x')$ on the surface mulitplied by the area of this surface, l^2. Similarly, the force on the surface at $x = x' + l$ is the traction $\boldsymbol{T}(x' + l)$ multiplied by the surface area l^2, allowing us to calculate the component of the resultant force on the cube due to stresses between opposite faces (figure 2.3):

$$\boldsymbol{F_x}(x') = l^2(\boldsymbol{T}(x' + l) - \boldsymbol{T}(x')). \tag{2.4}$$

Figure 2.3: The forces on a cube due to tractions on opposite faces.

A traction at position x can be written in terms of the stress tensor (using equation 2.3) as

$$\boldsymbol{T}(x) = \sigma \cdot \boldsymbol{e_x} = \sigma_{xx}(x)\boldsymbol{e_x} + \sigma_{xy}(x)\boldsymbol{e_y} + \sigma_{xz}(x)\boldsymbol{e_z}, \tag{2.5}$$

so to find the resultant force on the cube as a result of the tractions on every face, we calculate

$$\boldsymbol{F_x}(x') = l^2\left[\left(\sigma_{xx}(x'+l) - \sigma_{xx}(x')\right)\boldsymbol{e_x} + \left(\sigma_{xy}(x'+l) - \sigma_{xy}(x')\right)\boldsymbol{e_y} + \left(\sigma_{xz}(x'+l) - \sigma_{xz}(x')\right)\boldsymbol{e_z}\right]$$
$$= l^3\left[\frac{\sigma_{xx}(x'+l) - \sigma_{xx}(x')}{l}\boldsymbol{e_x} + \frac{\sigma_{xy}(x'+l) - \sigma_{xy}(x')}{l}\boldsymbol{e_y} + \frac{\sigma_{xz}(x'+l) - \sigma_{xz}(x')}{l}\boldsymbol{e_z}\right]. \tag{2.6}$$

Taking the limit $l \to 0$ turns allows us to turn the fractions into partial derivatives

$$\boldsymbol{F_x}(x') = l^3\left[\frac{\partial\sigma_{xx}}{\partial x}\bigg|_{x'}\boldsymbol{e_x} + \frac{\partial\sigma_{xy}}{\partial x}\bigg|_{x'}\boldsymbol{e_y} + \frac{\partial\sigma_{xz}}{\partial x}\bigg|_{x'}\boldsymbol{e_z}\right], \tag{2.7}$$

where the coefficient l^3 has been left in for continuity. This can be expressed more concisely using equation 2.3 as

$$\boldsymbol{F_x}(x') = l^3 \left(\frac{\partial \sigma}{\partial x}\bigg|_{x'} \cdot \boldsymbol{e_x} \right). \tag{2.8}$$

We neglect the evaluation at x' for simplicity and write this equation for the resultant force in three dimensions, by including a similar calculation for the y and z components,

$$\boldsymbol{F}_{Stress} = l^3 \left(\frac{\partial}{\partial x}\boldsymbol{e_x} + \frac{\partial}{\partial y}\boldsymbol{e_y} + \frac{\partial}{\partial z}\boldsymbol{e_z} \right) \cdot \sigma = l^3 \nabla \cdot \sigma. \tag{2.9}$$

In order to complete our conversion of Newton's second law to continuum form, we note that the mass of the cube is $m = l^3 \rho$, where ρ is the density of the material. We also note that for a body force per unit mass $\boldsymbol{B}$, the overall body force is

$$\boldsymbol{B}_{Body} = l^3 \rho \boldsymbol{B}, \tag{2.10}$$

and therefore by Newton's second law, $m\boldsymbol{a} = \boldsymbol{F}_{Stress} + \boldsymbol{B}_{Body}$, and cancelling the volume terms, we get the equation of motion for a solid

$$\boxed{\rho \boldsymbol{a} = \nabla \cdot \sigma + \rho \boldsymbol{B}} \tag{2.11}$$

which describes the motion of a material element due to the internal stresses in the material, and an external body force.

2.3 Symmetry of the stress tensor

So far, we have been able to derive an equation of motion for elastic materials, due to internal stresses described by the Cauchy stress tensor σ. The application of conservation laws to this equation of motion allows us to prove a fundamental property of the stress tensor, namely that it is symmetric.

Proposition 2.3.1. *If angular momentum is conserved then the Cauchy stress tensor σ is symmetric, that is $\sigma_{ij} = \sigma_{ji}$.*

Proof. Consider a material volume V bounded by a surface ∂V, and denote the position of a material element in the solid by the vector $\boldsymbol{u}$. The angular momentum of u is then equal to $\boldsymbol{u} \times \rho \frac{\partial \boldsymbol{u}}{\partial t}$. Conservation of angular momentum means that the rate of change of the total angular momentum of the material is equal to the sum of the moments of forces on the material

$$\frac{d}{dt} \int_V \boldsymbol{u} \times \rho \frac{\partial \boldsymbol{u}}{\partial t} \, dV = \int_{\partial V} \boldsymbol{u} \times (\sigma \cdot d\boldsymbol{S}) + \int_V \boldsymbol{u} \times \boldsymbol{F} \, dV, \tag{2.12}$$

where $\boldsymbol{F}$ is the body force on the material, and $\sigma \cdot d\boldsymbol{S}$ defines the force due to external tractions at each point on the surface of the material. Firstly, we bring the time derivative inside the integral on the left hand side of equation 2.12 by changing it from a total derivative to a partial derivative:

$$\begin{aligned}
\frac{d}{dt} \int_V \boldsymbol{u} \times \rho \frac{\partial \boldsymbol{u}}{\partial t} \, dV &= \int_V \frac{\partial}{\partial t} \left(\boldsymbol{u} \times \rho \frac{\partial \boldsymbol{u}}{\partial t} \right) \, dV \\
&= \int_V \frac{\partial \boldsymbol{u}}{\partial t} \times \rho \frac{\partial \boldsymbol{u}}{\partial t} + \boldsymbol{u} \times \rho \frac{\partial^2 \boldsymbol{u}}{\partial t^2} \, dV \\
&= \int_V \boldsymbol{u} \times \rho \frac{\partial^2 \boldsymbol{u}}{\partial t^2} \, dV.
\end{aligned} \tag{2.13}$$

Next, we rewrite the surface integral in equation 2.12 using the divergence theorem. In index notation,

$$
\begin{aligned}
\int_{\partial V} \left[\boldsymbol{u} \times (\sigma \cdot d\boldsymbol{S}) \right]_i &= \int_{\partial V} \epsilon_{ijk} x_j \sigma_{kl} n_l \, dS \\
&= \int_V \frac{\partial}{\partial x_l} \epsilon_{ijk} x_j \sigma_{kl} \, dV \\
&= \int_V \epsilon_{ijk} \left(\frac{\partial x_j}{\partial x_l} \sigma_{kl} + x_j \frac{\partial \sigma_{kl}}{\partial x_l} \right) dV \\
&= \int_V \epsilon_{ijk} \left(\delta_{jl} \sigma_{kl} + x_j \frac{\partial \sigma_{kl}}{\partial x_l} \right) dV \\
&= \int_V \epsilon_{ijk} \sigma_{kj} \, dV + \int_V \boldsymbol{u} \times (\nabla \cdot \sigma) \, dV.
\end{aligned}
\tag{2.14}
$$

Combining these two formulas allows us the rewrite equation 2.12 as

$$
\int_V \boldsymbol{u} \times \left(\rho \frac{\partial^2 \boldsymbol{u}}{\partial t^2} - \boldsymbol{F} - \nabla \cdot \sigma \right) dV = \int_V \epsilon_{ijk} \sigma_{kj} \, dV.
\tag{2.15}
$$

The term in brackets on the left hand side is equal to zero as it is just a rearranged form of the equation of motion (equation 2.11), so

$$
\int_V \epsilon_{ijk} \sigma_{kj} \, dV = 0.
\tag{2.16}
$$

This must hold for any volume V, therefore

$$
\begin{aligned}
\epsilon_{ijk} \sigma_{kj} = 0 &\iff \epsilon_{imn} \epsilon_{ijk} \sigma_{kj} = 0, \\
&\iff \left(\delta_{mj} \delta_{nk} - \delta_{mk} \delta_{nj} \right) \sigma_{kj} = 0, \\
&\iff \sigma_{nm} - \sigma_{mn} = 0.
\end{aligned}
\tag{2.17}
$$

$\square$

We now know that the stress tensor is symmetric. Next, we will study another symmetric tensor, the strain tensor, which describes the elastic deformation in the material, and discuss how the relationship between these two tensors defines the elastic properties of the material.

2.4   The strain tensor

To take our study of linear elasticity further, we must find a way to describe the strain of a material at any point in terms of the displacements of material elements at that point. We consider the case of some arbitrary 3 dimensional deformation, where matter will not only be stretched but also rotated and sheared. We model this by a deformation of every point of material in the solid, i.e. a translation at each point, where the translation depends on the coordinates.

Consider a material element at a point given by the position

$$
\boldsymbol{x} = \begin{bmatrix} x \\ y \\ z \end{bmatrix}.
\tag{2.18}
$$

If the solid is deformed continuously, then after deformation the point $\boldsymbol{x}$ will have moved to the point

$$\boldsymbol{x}' = \begin{bmatrix} x + u(x,y,z) \\ y + v(x,y,z) \\ z + w(x,y,z) \end{bmatrix}, \tag{2.19}$$

where the functions u, v and w collectively describe the 3 dimensional displacement of the material element at $\boldsymbol{x} = (x,y,z)$. Now if we look at a material element at the point $\boldsymbol{x}+\delta\boldsymbol{x}$, where

$$\boldsymbol{x} + \delta\boldsymbol{x} = \begin{bmatrix} x + \delta x \\ y + \delta y \\ z + \delta z \end{bmatrix}, \tag{2.20}$$

then after the deformation given by u, v and w, the material at $\boldsymbol{x} + \delta\boldsymbol{x}$ will move to

$$\boldsymbol{x}' + \delta\boldsymbol{x}' = \begin{bmatrix} x + \delta x + u(x + \delta x, y + \delta y, z + \delta z) \\ y + \delta y + v(x + \delta x, y + \delta y, z + \delta z) \\ z + \delta z + w(x + \delta x, y + \delta y, z + \delta z) \end{bmatrix}. \tag{2.21}$$

We can take the Taylor expansion of u, v and w, and if we assume that δx, δy and δz are very small then we only need to keep the first order terms:

$$\boldsymbol{x}' + \delta\boldsymbol{x}' \approx \begin{bmatrix} x + \delta x + u(x,y,z) + \frac{\partial u}{\partial x}\delta x + \frac{\partial u}{\partial y}\delta y + \frac{\partial u}{\partial z}\delta z \\ y + \delta y + v(x,y,z) + \frac{\partial w}{\partial x}\delta x + \frac{\partial w}{\partial y}\delta y + \frac{\partial w}{\partial z}\delta z \\ z + \delta z + w(x,y,z) + \frac{\partial u}{\partial v}\delta x + \frac{\partial v}{\partial y}\delta y + \frac{\partial v}{\partial z}\delta z \end{bmatrix}. \tag{2.22}$$

Subtracting equation 2.19 allows us to rewrite the term $\delta\boldsymbol{x}'$ as a matrix transformation:

$$\delta\boldsymbol{x}' = \begin{bmatrix} 1 + \frac{\partial u}{\partial x} & \frac{\partial u}{\partial y} & \frac{\partial u}{\partial z} \\ \frac{\partial v}{\partial x} & 1 + \frac{\partial v}{\partial y} & \frac{\partial v}{\partial z} \\ \frac{\partial w}{\partial x} & \frac{\partial w}{\partial y} & 1 + \frac{\partial w}{\partial z} \end{bmatrix} \begin{bmatrix} \delta x \\ \delta y \\ \delta z \end{bmatrix} = (I_3 + M)\,\delta\boldsymbol{x}. \tag{2.23}$$

In this equation, M is called the *deformation matrix*. To allow for more compact notation, we define $x_1 = x, x_2 = y, x_3 = z$ and $u_1 = u, u_2 = v, u_3 = w$, so that

$$M_{ij} = \frac{\partial u_i}{\partial x_j}. \tag{2.24}$$

Our next step is to separate the deformation matrix M into a symmetric and anti-symmetric part, recalling from linear algebra that any arbitrary matrix can be written as the sum of a symmetric matrix and an anti-symmetric matrix. To do this we write M as

$$M = \begin{bmatrix} \frac{\partial u}{\partial x} & \frac{1}{2}\left(\frac{\partial u}{\partial y} + \frac{\partial v}{\partial x}\right) + \frac{1}{2}\left(\frac{\partial u}{\partial y} - \frac{\partial v}{\partial x}\right) & \frac{1}{2}\left(\frac{\partial u}{\partial z} + \frac{\partial w}{\partial x}\right) + \frac{1}{2}\left(\frac{\partial u}{\partial z} - \frac{\partial w}{\partial x}\right) \\ \frac{1}{2}\left(\frac{\partial v}{\partial x} + \frac{\partial u}{\partial y}\right) + \frac{1}{2}\left(\frac{\partial v}{\partial x} - \frac{\partial u}{\partial y}\right) & \frac{\partial v}{\partial y} & \frac{1}{2}\left(\frac{\partial v}{\partial z} + \frac{\partial w}{\partial y}\right) + \frac{1}{2}\left(\frac{\partial v}{\partial z} - \frac{\partial w}{\partial y}\right) \\ \frac{1}{2}\left(\frac{\partial w}{\partial x} + \frac{\partial u}{\partial z}\right) + \frac{1}{2}\left(\frac{\partial w}{\partial x} - \frac{\partial u}{\partial x}\right) & \frac{1}{2}\left(\frac{\partial w}{\partial y} + \frac{\partial v}{\partial z}\right) + \frac{1}{2}\left(\frac{\partial w}{\partial y} - \frac{\partial v}{\partial z}\right) & \frac{\partial w}{\partial z} \end{bmatrix}. \tag{2.25}$$

We then split M into $M = E + R$, where E and R are the symmetric and anti-symmetric part of this matrix respectively:

$$E = \begin{bmatrix} e_{11} & \frac{1}{2}e_{12} & \frac{1}{2}e_{13} \\ \frac{1}{2}e_{12} & e_{22} & \frac{1}{2}e_{23} \\ \frac{1}{2}e_{13} & \frac{1}{2}e_{23} & e_{33} \end{bmatrix} \quad \text{with} \quad e_{ii} = \frac{\partial u_i}{\partial x_i}, \quad e_{ij} = \frac{\partial u_i}{\partial x_j} + \frac{\partial u_j}{\partial x_i}, \tag{2.26}$$

and

$$R = \begin{bmatrix} 0 & -\omega_3 & \omega_2 \\ \omega_3 & 0 & -\omega_1 \\ -\omega_2 & \omega_1 & 0 \end{bmatrix} \quad \text{with} \quad \omega_i = \frac{1}{2}\epsilon_{ijk}\frac{\partial u_j}{\partial x_i}. \tag{2.27}$$

Note that R here is a rotation matrix, so the matrix E contains the true deformation: the elements e_{ii} correspond to a stretching or compression along the main axis while e_{ij} corresponds to a local shear. This leads us to define the rotation-less part of the deformation, E, as the strain tensor.

Definition 2.4.1 (Strain Tensor). Consider an elastic deformation given by the transformation $\boldsymbol{x} \longrightarrow \boldsymbol{x'} = \boldsymbol{x} + \boldsymbol{u}$, where the deformation $\boldsymbol{u}$ is a vector field defined at every point $\boldsymbol{x}$ in the material. The *strain tensor* is the symmetric part of the deformation matrix $M_{ij} = \frac{\partial u_i}{\partial x_j}$, that is, the matrix E where

$$E_{ij} = \tfrac{1}{2}\left(\frac{\partial u_i}{\partial x_j} + \frac{\partial u_j}{\partial x_i}\right), \quad \text{(equation 2.26)}.$$

The *strain-displacement equations* can be rewritten in vector form:

$$\boxed{E = \frac{1}{2}\left[\nabla\boldsymbol{u} + (\nabla\boldsymbol{u})^T\right]} \tag{2.28}$$

2.5   Hooke's Law

So far we have defined the stress and strain of a material as two 3×3 matrices called the stress tensor and the strain tensor. To take our study of linear elasticity further and begin to model the elastic properties of solids we must find a way to relate these two tensors. To do this, we use a method inspired a Hooke's Law, an simple equation that we are all familiar with from introductory mechanics classes.

Hooke's Law states that the relationship between the force F applied to a spring and the extension of the spring Δx is linear, i.e.

$$F = k\,\Delta x \tag{2.29}$$

This relationship only remains linear for small forces and extensions; at larger applied forces and extensions the relation becomes much more complicated. For our purposes, however, this relationship should still hold because we are only studying small elastic stresses and displacements. Consequently, we theorise that the relationship between the stress tensor and the strain tensor is linear. As both the stress and strain tensors are rank 2 (that is, they are 3×3 matrices), for the relationship to be linear they must be related by a rank 4 tensor of proportionality:

$$\boxed{\sigma_{ij} = A_{ijkl}E_{kl}}$$

Here A is the rank 4 tensor known as the *stiffness tensor*, and this equation gives the so-called constitutive relation for the stress and strain of the material [14].

2.6 Elasticity in isotropic materials

We now develop this relation further for the case of an isotropic material (that is, a material that is the same in every direction). If we disregard any constraints on the stiffness tensor A_{ijkl} then this rank 4 tensor can have at most 81 independent elements ($3 \times 3 \times 3 \times 3$). However, as both the stress tensor σ and the strain tensor E are symmetric, we can place a further restriction on the number of elements of A_{ijkl}.

Proposition 2.6.1. *If two tensors of rank 2 are related by a linear map given by the rank 4 tensor A_{ijkl}, and both rank 2 tensors are symmetric, then the tensor A_{ijkl} has at most 36 independent elements.*

Proof. Consider first the symmetry of E. We have $E_{kl} = E_{lk}$, so

$$\sigma_{ij} = A_{ijkl}E_{kl} = A_{ijkl}E_{lk} = A_{ijlk}E_{kl}, \tag{2.30}$$

therefore $A_{ijkl} = A_{ijlk}$.

Next, consider the symmetry of σ. We have $\sigma_{ij} = \sigma_{ji}$, so

$$\sigma_{ji} = A_{ijkl}E_{kl} = \sigma_{ij} = A_{jikl}E_{kl}, \tag{2.31}$$

so it follows that $A_{ijkl} = A_{jikl}$.

If we ignore k and l, then there are possible values of A_{ijkl} so that $A_{ijkl} = A_{jikl}$. Similarly, if we ignore i and j then there are 6 possible values such that $A_{ijkl} = A_{ijlk}$. As a result there are $6 \times 6 = 36$ independent elements of the tensor A_{ijkl}. $\qquad\square$

Therefore, in the case of any material either isotropic or anisotropic, the stiffness tensor A_{ijkl} must have at most 36 independent elements. If we consider only isotropic materials, this number can be narrowed down further to only two. To begin with, we recall from linear algebra that all symmetric real matrices can be diagonalized through an appropriate choice of basis, allowing us to write the strain tensor E in diagonal form. This makes sense physically as the material is isotropic, so we can pick our coordinate axes arbitrarily such that E is diagonal. Furthermore, using the fact that the material is isotropic we can assume that the principal axes of the stress and strain tensors are coincident, and therefore if E is diagonal then σ must also be diagonal. This means that we now only need to consider 9 elements of A_{ijkl},

$$\begin{aligned}
\sigma_{11} &= A_{1111}E_{11} + A_{1122}E_{22} + A_{1133}E_{33}, \\
\sigma_{22} &= A_{2211}E_{11} + A_{2222}E_{22} + A_{2233}E_{33}, \\
\sigma_{33} &= A_{3311}E_{11} + A_{3322}E_{22} + A_{3333}E_{33}.
\end{aligned} \tag{2.32}$$

Since the material is isotropic, the relationship between normal stresses and straines oriented in the same directions should be the same in all directions, implying that $A_{1111} = A_{2222} = A_{3333} = A_d$. Furthermore, the relationship between a normal stress in one direction and a strain in another direction should also be the same in every direction, so $A_{1122} = A_{1133} = A_{2211} = A_{2233} = A_{3311} = A_{3322} = A_0$ We can then rewrite the relation between the diagonalized stress and strain tensors as

$$\sigma_{11} = (A_d - A_0) E_{11} + A_0 (E_{11} + E_{22} + E_{33}),$$
$$\sigma_{11} = (A_d - A_0) E_{22} + A_0 (E_{11} + E_{22} + E_{33}),$$
$$\sigma_{11} = (A_d - A_0) E_{33} + A_0 (E_{11} + E_{22} + E_{33}), \qquad (2.33)$$
$$\text{or,}$$
$$\sigma_{ij} = (A_d - A_0) E_{ij} + A_0 \delta_{ij} E_{kk},$$

which we can rewrite as

$$\sigma_{ij} = \lambda \delta_{ij} E_{kk} + 2\mu E_{ij}, \qquad (2.34)$$

where λ and μ are two physical parameters called the *Lamé coefficients*. The parameter λ represents the ability of the material to be stretched, and the parameter μ represents the ability of the material to be sheared [14] [15].

We now need to express E as a function of σ. To do this, we begin by taking the trace of the previous equation to relate the trace of σ to the trace of E:

$$
\begin{aligned}
\text{Tr}(\sigma) = \sum_{i=1}^{3} \sigma_{ii} &= \sum_{i=1}^{3} \left[\lambda \sum_{k=1}^{3} E_{kk} + 2\mu E_{ii} \right] \\
&= \sum_{i=1}^{3} \left[\lambda (E_{11} + E_{22} + E_{33}) + 2\mu E_{ii} \right] \\
&= 3\lambda (E_{11} + E_{22} + E_{33}) + 2\mu (E_{11} + E_{22} + E_{33}) \\
&= (3\lambda + 2\mu) \sum_{i=1}^{3} E_{ii} \\
&= (3\lambda + 2\mu) \text{Tr}(E).
\end{aligned}
\qquad (2.35)
$$

This relation can be rewritten as

$$E_{kk} = \sum_{i=1}^{3} E_{kk} = \text{Tr}(E) = \frac{\text{Tr}(E)}{3\lambda + 2\mu} = \frac{\sum_{i=1}^{3} \sigma_{kk}}{3\lambda + 2\mu} = \frac{\sigma_{kk}}{3\lambda + 2\mu}, \qquad (2.36)$$

Substituting this into equation 2.34 gives

$$\sigma_{ij} = \lambda \delta_{ij} \frac{\sigma_{kk}}{3\lambda + 2\mu} + 2\mu E_{ij},$$
$$\text{so} \qquad (2.37)$$
$$E_{ij} = \frac{\sigma_{ij}}{2\mu} - \frac{\lambda}{2\mu (3\lambda + 2\mu)} \delta_{ij} \sigma_{kk}.$$

The two alternate forms of this relation can be used to calculate derive the an equation for the dynamics of isotropic material subject to internal stresses.

2.7 The Navier-Cauchy equation

The Navier-Cauchy equation (sometimes called the Navier or Navier-Lamé equation) [16] describes the dynamics of an isotropic, linearly elastic material. Clearly, in order to derive an equation for this specific case, we must start from the equation of motion for stresses and displacements that was derived in section 2.2 (equation 2.11),

$$\rho\boldsymbol{a} = \nabla \cdot \sigma, \tag{2.38}$$

neglecting the body force for simplicity. The acceleration term is just a second partial derivative, and we can insert equation 2.34 to get

$$
\begin{aligned}
\rho\frac{\partial^2 u_i}{\partial t^2} &= \frac{\partial \sigma_{ij}}{\partial x_j} \\
&= \frac{\partial}{\partial x_j}\Big[\lambda\delta_{ij}E_{kk} + 2\mu E_{ij}\Big] \\
&= \frac{\partial}{\partial x_j}\left[\lambda\delta_{ij}\frac{\partial u_k}{\partial x_k} + \mu\left(\frac{\partial u_i}{\partial x_j} + \frac{\partial u_j}{\partial x_i}\right)\right] \\
&= (\lambda + \mu)\frac{\partial^2 u_j}{\partial x_i\partial x_j} + \mu\frac{\partial^2 u_i}{\partial x_j^2}.
\end{aligned}
\tag{2.39}
$$

In vector form, this equation, the Navier-Cauchy equation, is written as

$$\boxed{\rho\frac{\partial^2 \boldsymbol{u}}{\partial t^2} = (\lambda + \mu)\nabla\left(\nabla \cdot \boldsymbol{u}\right) + \mu\nabla^2\boldsymbol{u}} \tag{2.40}$$

The solutions to this equation describe the time evolution of displacements in the material.

2.8 Energies of deformation

In order to derive differential equations to describe the elastic vibrations of different bodies, we begin by writing an equation for the Lagrangian (kinetic energy minus potential energy) of an elastic material.

The kinetic energy of an elastic deformation $\boldsymbol{u}$ in an elastic material of uniform density ρ in a volume $D \in \mathbb{R}^3$ is clearly given by

$$\boxed{T = \int_D \frac{\rho}{2}\left|\frac{\partial \boldsymbol{u}}{\partial t}\right|^2 dV = \int_D \frac{\rho}{2}\left(\frac{\partial u_k}{\partial t}\right)^2 dV} \tag{2.41}$$

To compute the potential energy we must evaluate the work performed by all the surface forces to perform a deformation (assuming no body forces are acting on the elastic material). The work done by a force on a surface is the integral force multiplied by the distance travelled at every point on the surface. We use here the *principle of virtual work* [14]. For some infinitesimally small *virtual deformation* $\delta\boldsymbol{u}$, the *virtual work* is defined to be the work done by the forces on each material element through the virtual displacement

$$\delta W = \int_{\partial D}(\delta\boldsymbol{u} \cdot \sigma)d\boldsymbol{A} = \int_{\partial D}\delta u_i\sigma_{ij}n_j dA. \tag{2.42}$$

We can then use the divergence theorem to transform this surface integral into a volume integral

$$\delta W = \int_{\partial D} (\delta \boldsymbol{u} \cdot \sigma) d\boldsymbol{A} = \int_D \nabla \cdot (\delta \boldsymbol{u} \cdot \sigma) dV$$

$$= \int_D \frac{\partial}{\partial x_j} (\delta u_i \sigma_{ij}) dV \qquad (2.43)$$

$$= \int_D \left(\frac{\partial \delta u_i}{\partial x_j} \sigma_{ij} + \frac{\partial \sigma_{ij}}{\partial x_j} \delta u_i \right) dV.$$

We can once again use the equation of motion for deformations in an elastic body

$$\rho \boldsymbol{a} = \nabla \cdot \sigma \iff \rho \frac{\partial^2 u_i}{\partial t^2} = \frac{\partial \sigma_{ij}}{\partial x_j}, \qquad (2.44)$$

to rewrite our expression for the virtual work

$$\delta W = \int_D \left(\frac{\partial \delta u_i}{\partial x_j} \sigma_{ij} + \rho \frac{\partial^2 u_i}{\partial t^2} \delta u_i \right) dV$$

$$= \int_D \left(\frac{\partial \delta u_i}{\partial x_j} \sigma_{ij} + \frac{\rho}{2} \frac{\partial u_i}{\partial t} \frac{\partial^2 u_i}{\partial t^2} \delta t \right) dV$$

$$= \int_D \left(\frac{\partial \delta u_i}{\partial x_j} \sigma_{ij} + \frac{\rho}{2} \frac{\partial}{\partial t} \left(\frac{\partial u_i}{\partial t} \right)^2 \delta t \right) dV \qquad (2.45)$$

$$= \int_D \left(\frac{\partial \delta u_i}{\partial x_j} \sigma_{ij} + \frac{\rho}{2} \delta \left(\frac{\partial u_i}{\partial t} \right)^2 \right) dV.$$

Recall from section 2.4 that the derivative $\frac{\partial u_i}{\partial x_j}$ defines the deformation tensor M_{ij}, which can be separated into the symmetric strain matrix E_{ij} and the antisymmetric rotation matrix R_{ij} by $M_{ij} = E_{ij} + R_{ij}$. Furthermore, we can assert the fact that the product $R_{ij}\sigma_{ij} = 0$. To prove this we use the symmetry of σ and antisymmetry of R, so

$$2R_{ij}\sigma_{ij} = R_{ij}\sigma_{ij} + R_{ij}\sigma_{ij}$$

$$= R_{ij}\sigma_{ij} + R_{ij}\sigma_{ji}$$

$$= R_{ij}\sigma_{ij} + R_{ji}\sigma_{ij}$$

$$= R_{ij}\sigma_{ij} - R_{ij}\sigma_{ij} \qquad (2.46)$$

$$= 0,$$

$$\text{therefore } R_{ij}\sigma_{ij} = 0.$$

Then expanding out term $\frac{\partial \delta u_i}{\partial x_j} = \delta M_{ij}$ in our expression for the work done in the deformation gives

$$\delta W = \int_D \left(\delta M_{ij} \sigma_{ij} + \frac{\rho}{2} \delta \left(\frac{\partial u_i}{\partial t} \right)^2 \right) dV,$$

$$= \int_D \left((\delta E_{ij} + \delta R_{ij}) \sigma_{ij} + \frac{\rho}{2} \delta \left(\frac{\partial u_i}{\partial t} \right)^2 \right) dV, \qquad (2.47)$$

$$= \int_D \left(\delta E_{ij} \sigma_{ij} + \frac{\rho}{2} \delta \left(\frac{\partial u_i}{\partial t} \right)^2 \right) dV.$$

Furthermore, from section 2.6 we have that for an isotropic elastic medium, $\sigma_{ij} = \lambda \delta_{ij} E_{kk} + 2\mu E_{ij}$, so

$$E_{ij}\sigma_{ij} = E_{ij}(\lambda\delta_{ij}E_{kk} + 2\mu E_{ij})$$
$$= \lambda E_{ii}E_{kk} + 2\mu E_{ij}^2 \tag{2.48}$$
$$= \lambda E_{kk}^2 + 2\mu E_{ij}^2.$$

Allowing us to write

$$\delta E_{ij}\sigma_{ij} = \delta E_{ij}(\lambda\delta_{ij}E_{kk} + 2\mu E_{ij})$$
$$= \lambda\delta E_{ii}E_{kk} + 2\mu\delta E_{ij}E_{ij}$$
$$= \lambda\frac{\delta(E_{kk})^2}{2} + 2\mu\frac{\delta(E_{ij}^2)}{2} \tag{2.49}$$
$$= \frac{\delta}{2}\left(\lambda E_{kk}^2 + 2\mu E_{ij}^2\right)$$
$$= \frac{\delta}{2}(E_{ij}\sigma_{ij}).$$

Therefore for the virtual work,

$$\delta W = \frac{\delta}{2}\int_D\left(E_{ij}\sigma_{ij} + \rho\left(\frac{\partial u_i}{\partial t}\right)^2\right)dV. \tag{2.50}$$

This allows us to write an expression for the *total work*,

$$W = \frac{1}{2}\int_D\left(E_{ij}\sigma_{ij} + \rho\left(\frac{\partial u_i}{\partial t}\right)^2\right)dV. \tag{2.51}$$

The second term in the integral here obviously represents kinetic energy. What this equation for total work is *actually* describing is how when work is done on a body to cause a deformation, the energy is converted to both potential and kinetic energy. This allows us to conclude that the first term in the integral must be describing the potential energy V gained through the deformation, that is,

$$V = \frac{1}{2}\int_D E_{ij}\sigma_{ij}dV$$
$$= \frac{1}{2}\int_D \lambda E_{kk}^2 + 2\mu E_{ij}^2 dV. \tag{2.52}$$

We also recall from section 2.4 that

$$E = \frac{1}{2}\left[\nabla\boldsymbol{u} + (\nabla\boldsymbol{u})^T\right] \iff E_{ij} = \frac{1}{2}\left(\frac{\partial u_i}{\partial x_j} + \frac{\partial u_j}{\partial x_i}\right),$$
$$\implies E_{kk} = \frac{\partial u_k}{\partial x_k}. \tag{2.53}$$

This then allows us to write explicitly an equation for the potential energy gained due to the deformation $\boldsymbol{u}$.

$$\boxed{V = \int_D \frac{1}{2}\left(\lambda\left(\frac{\partial u_k}{\partial x_k}\right)^2 + \frac{\mu}{2}\left(\frac{\partial u_i}{\partial x_j} + \frac{\partial u_j}{\partial x_i}\right)^2\right)dV} \tag{2.54}$$

2.9 Action for an isotropic elastic medium

We have equation 2.44 describing the kinetic energy $T(\boldsymbol{u})$ for an elastic deformation $\boldsymbol{u}$,

$$T(\boldsymbol{u}) = \int_D \frac{\rho}{2} \left(\frac{\partial u_k}{\partial t} \right)^2 dV, \tag{2.55}$$

and the equation for the potential energy $V(\boldsymbol{u})$,

$$V(\boldsymbol{u}) = \int_D \frac{1}{2} \left(\lambda \left(\frac{\partial u_k}{\partial x_k} \right)^2 + \frac{\mu}{2} \left(\frac{\partial u_i}{\partial x_j} + \frac{\partial u_j}{\partial x_i} \right)^2 \right) dV, \tag{2.56}$$

so we can then write an expression for the Lagrangian $L = T - V$

$$L(\boldsymbol{u}) = \int_D \frac{\rho}{2} \left(\frac{\partial u_k}{\partial t} \right)^2 - \frac{1}{2} \left(\lambda \left(\frac{\partial u_k}{\partial x_k} \right)^2 + \frac{\mu}{2} \left(\frac{\partial u_i}{\partial x_j} + \frac{\partial u_j}{\partial x_i} \right)^2 \right) dV. \tag{2.57}$$

The action is then defined to be integral over the trajectory of the deformation $\boldsymbol{u}(t)$ from time $t = 0$ to some final time $t = T$

$$S(\boldsymbol{u}) = \int_0^T L(\boldsymbol{u}(t)) dt. \tag{2.58}$$

This allows us to write down the action for a deformation in an isotropic elastic medium.

$$\boxed{S(\boldsymbol{u}) = \int_0^T \int_D \frac{\rho}{2} \left(\frac{\partial u_k}{\partial t} \right)^2 - \frac{1}{2} \left(\lambda \left(\frac{\partial u_k}{\partial x_k} \right)^2 + \frac{\mu}{2} \left(\frac{\partial u_i}{\partial x_j} + \frac{\partial u_j}{\partial x_i} \right)^2 \right) dV \, dt} \tag{2.59}$$

From the Lagrangian L given above, we can use the Euler-Lagrange equations to derive equations of motion for the elastic deformation $\boldsymbol{u}(x, y, z, t)$ in the material given by $D \in \mathbb{R}^3$. The advantage of the action formulation is that expanding out variations in the action, and setting this variation to zero through Hamilton's *principle of least action* allows us to derive relevant boundary conditions for our system along with the equations of motion.

Chapter 3

The Bowed String

In the introduction, we discussed Helmholtz's experimental observations for the dynamics of the bowed string. The theory of elasticity can be used to derive the *wave equation* for the motion of the string. We will then impose that due to the slip-stick action of the bow, the solutions to this equation must follow a saw-toothed pattern, as seen in Helmholtz's observation given in figure 1.4. Using this behaviour, along with well-known properties of the solutions to the wave equation, we will derive the spectrum of frequencies of the bowed string, and show that the motion of the string at any point must be bounded by a parabolic shape, as shown in figure 1.5. This section follows David J. Benson's *"Music: A Mathematical Offering"* [3].

3.1   The stretched string

We consider a stretched string. The string is stretched so that $u_1(L - l) = l$, and we consider the deformations to lie entirely within the x_1, x_2 (or x, y) plane, so $u_3 = 0$. The string is very thin, so $\frac{du_1}{dx_2} = \frac{du_2}{dx_2} = 0$. Recalling the Navier-Cauchy equation (2.40),

$$\rho \frac{\partial^2 \boldsymbol{u}}{\partial t^2} = (\lambda + \mu) \nabla (\nabla \cdot \boldsymbol{u}) + \mu \nabla^2 \boldsymbol{u}, \tag{3.1}$$

we can use these simplifications to write down differential equations to describe the deformations of the stretched string. We have

$$\rho \frac{\partial^2 u_1}{\partial t^2} = (\lambda + 2\mu) \frac{\partial^2 u_1}{\partial x^2}, \tag{3.2}$$

$$\rho \frac{\partial^2 u_2}{\partial t^2} = \mu \frac{\partial^2 u_2}{\partial x^2}. \tag{3.3}$$

The second of these two equations describes the transverse oscillations of the string. If we set $u_2(x, t) = y(x, t)$, then this equation is simply the wave equation

$$\boxed{\frac{\partial^2 y}{\partial t^2} = c^2 \frac{\partial^2 y}{\partial x^2}} \tag{3.4}$$

for waves on the string with wave speed given by

$$c = \sqrt{\frac{\mu}{\rho}}, \tag{3.5}$$

where ρ is the volume density of the string and μ is Lamé's second parameter, the *shear modulus*. This makes sense - transverse oscillations on a string are shear waves.

3.2 The wave equation

In order to solve the wave equation (3.4) to describe the Helmholtz patterns formed on bowed strings, we first must find the most general form of the solution to the wave equation subject to the boundary conditions that the string must be fixed at both ends. The most general form of the solution to the wave equation is given by d'Alembert's theorem [3]:

Theorem 3.2.1 (d'Alembert's Theorem). *The general solution to the wave equation*

$$\frac{\partial^2 y}{\partial t^2} = c^2 \frac{\partial^2 y}{\partial x^2}$$

is given by

$$y = f(x + ct) - g(x - ct)$$

The solutions satisfying the boundary conditions $y = 0$ for $x = 0$ and $x = l$ for all values of t, are of the form

$$y = f(x + ct) - f(-x + ct)$$

where f satisfies $f(\lambda) = f(\lambda + 2l)$ for all values of λ.

Proof. We begin by factorising the operator

$$\frac{\partial^2}{\partial t^2} - c^2 \frac{\partial^2}{\partial x^2} = \left(\frac{\partial}{\partial t} + c \frac{\partial}{\partial x} \right) \left(\frac{\partial}{\partial t} - c \frac{\partial}{\partial x} \right). \tag{3.6}$$

We then make the change of variables

$$u = x + ct, \qquad v = x - ct. \tag{3.7}$$

By the multivariate chain rule,

$$\frac{\partial y}{\partial t} = \frac{\partial y}{\partial u} \frac{\partial u}{\partial t} + \frac{\partial y}{\partial v} \frac{\partial v}{\partial t} = c \frac{\partial y}{\partial u} - c \frac{\partial y}{\partial v}. \tag{3.8}$$

Differentiating again gives

$$\begin{aligned}
\frac{\partial^2 y}{\partial t^2} = \frac{\partial}{\partial t} \frac{\partial y}{\partial t} &= \frac{\partial}{\partial u} \frac{\partial y}{\partial t} \frac{\partial u}{\partial t} + \frac{\partial}{\partial u} \frac{\partial y}{\partial t} \frac{\partial v}{\partial t} \\
&= c \left(c \frac{\partial^2 y}{\partial u^2} - c \frac{\partial^2 y}{\partial u \partial v} \right) - c \left(c \frac{\partial^2 y}{\partial v \partial u} - c \frac{\partial^2 y}{\partial v^2} \right) \\
&= c^2 \left(\frac{\partial^2 y}{\partial u^2} - 2 \frac{\partial^2 y}{\partial u \partial v} + \frac{\partial^2 y}{\partial v^2} \right).
\end{aligned} \tag{3.9}$$

A similar derivation shows that

$$\begin{aligned}
\frac{\partial y}{\partial x} &= \frac{\partial y}{\partial u} \frac{\partial u}{\partial x} + \frac{\partial y}{\partial v} \frac{\partial v}{\partial x} = \frac{\partial y}{\partial u} + \frac{\partial y}{\partial v}, \\
\frac{\partial^2 y}{\partial x^2} &= \frac{\partial^2 y}{\partial u^2} + 2 \frac{\partial^2 y}{\partial u \partial v} + \frac{\partial^2 y}{\partial v^2}.
\end{aligned} \tag{3.10}$$

Inserting this into the wave equation shows that

$$c^2 \left(\frac{\partial^2 y}{\partial u^2} - 2 \frac{\partial^2 y}{\partial u \partial v} + \frac{\partial^2 y}{\partial v^2} \right) = c^2 \left(\frac{\partial^2 y}{\partial u^2} + 2 \frac{\partial^2 y}{\partial u \partial v} + \frac{\partial^2 y}{\partial v^2} \right), \tag{3.11}$$

or,

$$\frac{\partial^2 y}{\partial u \partial v} = 0. \tag{3.12}$$

Integrating this directly shows the general solution to the wave equation is given by $y = f(u) = g(v)$, or with respect to x and t,

$$\boxed{y = f(x + ct) - g(x - ct)} \tag{3.13}$$

We now impose the boundary conditions that $y = 0$ at $x = 0$ and $x = l$. Beginning by setting $x = 0$, we find that

$$f(ct) - g(-ct) = 0 \tag{3.14}$$

for all values of t. Setting $\eta = ct$, we find that for all values of η,

$$f(\eta) = g(-\eta). \tag{3.15}$$

Thus,

$$y = f(x + ct) - f(-x + ct). \tag{3.16}$$

Substituting the other boundary condition, $y = 0$ at $x = l$, shows that

$$f(l + ct) - f(-l + ct) = 0, \tag{3.17}$$

for all t. This time substituting $\lambda = ct - l$, we find that for all λ,

$$f(\lambda) = f(\lambda + 2l). \tag{3.18}$$

$\square$

3.3 Fourier series

In order to write down the form of the solutions to the wave equation that match the jagged, saw-tooth pattern found by Helmoltz, we need to find some way to write an arbitrary periodic function in terms of simpler functions that we *can* describe explicitly, such as trigonometric functions. Fourier series provide a method for doing this, and in this section we will briefly outline the key results that will be used in this chapter. Further details are not crucial for this report and will be left to the appendix. The following theorem is taken from a set of first year calculus lectures, and will be quoted directly [17].

Theorem 3.3.1 (Sine-cosine Fourier expansion). *Consider a function f(x) of period 2L. The function can always be expressed in the form*

$$f(x) = \frac{a_0}{2} + \sum_{n=1}^{\infty} \left(a_n \cos\left(\frac{n\pi x}{L}\right) + b_n \sin\left(\frac{n\pi x}{L}\right) \right) \tag{3.19}$$

where a_0, a_n, b_n are constants labelled by the positive integer n, and are called the Fourier coefficients of f(x). If these Fourier coefficients are such that this series converges then it is called the Fourier series of f(x).

Proof. See appendix A.

It is also possible to write the Fourier series in terms of amplitudes and phases of a single trigonometric function, which is sometimes more convenient for a particular problem.

Corollary 3.3.2 (Phase-amplitude Fourier expansion). *Consider a function f(x) of period 2L which is given on the interval $(-L, L)$. Then its Fourier series can alternatively be expressed in the form*

$$f(x) = \frac{a_0}{2} + \sum_{n=1}^{\infty} \left(a_n \cos\left(\frac{n\pi x}{L} + \phi_n\right) \right) \tag{3.20}$$

for particular coefficients a_0, a_n.

Proof. See appendix A.

We also state here the method for calculating the Fourier coefficients for a given periodic function $f(x)$.

Lemma 3.3.3 (Fourier coefficients). *The Fourier coefficients a_n and b_n for periodic function with period $2L$ defined in the interval (0,2L) are given by*

$$a_n = \frac{1}{L} \int_0^L \cos\left(\frac{n\pi x}{L}\right) f(x) dx, \qquad b_n = \frac{1}{L} \int_0^L \sin\left(\frac{n\pi x}{L}\right) f(x) dx. \qquad (3.21)$$

Proof. See appendix A.

3.4   Helmholtz motion

As was discussed in section 1.2, under the action of bowing, the string alternates between sticking to and slipping against the string. At any point x_0 on the string, the string is either displaced with the bow at constant speed, or slips back against the bow at a different constant speed, leading to the zig-zagged pattern shown in figure 1.4. Furthermore, the motion of the apex of the waveform must be prescribed by a parabola.

We need to formulate this problem mathematically. We are looking for solutions $y(x,t)$ to the wave equation obeying the boundary conditions $y(0,t) = y(l,t) = 0$. At a particular value x_0 of x, the function $y(x_0,t)$ must be bounded for all t by a parabola defined as a function of x_0. The prescribed motion at x_0 must have periodicity $2l/c$,

$$y(x_0, t + \frac{2l}{c}) = y(x_0, t). \qquad (3.22)$$

This periodic function must follow the zig-zag pattern shown in section 1.2 at every point x_0.

We can try to solve the wave equation for this prescribed function $y(x_0, t)$ using d'Alembert's form of the solution to the wave equation. For some function $f(x_0, t)$ with $f(\lambda) = f(\lambda + 2l)$, we will have

$$y(x_0, t) = f(x_0 + ct) - f(-x_0 + ct). \qquad (3.23)$$

Considering the point $x_0 = l/2$, we get

$$y(l/2, t) = f(l/2 + ct) - f(-l/2 + ct). \qquad (3.24)$$

Next, at a time $t + l/c$, and at $x_0 = l/2$, the value of the function will be

$$y(l/2, t + l/c) = f(3l/2 + ct) - f(l/2 + ct). \qquad (3.25)$$

Adding these two equations together gives

$$y(l/2, t + l/c) + y(l/2, t) = f(3l/2 + ct) - f(-l/2 + ct). \qquad (3.26)$$

But $f(\lambda)$ is periodic with periodicity 2λ, so $f(3l/2 + ct) = f(-l/2 + ct)$. This gives us the equation

$$y(l/2, t + l/c) = -y(l/2, t). \qquad (3.27)$$

This tells us that the prescribed function $y(x_0, t)$ must be half period anti-symmetric at $x_0 = l/2$; that is, the function has periodicity $2l/c$, but must also take on an negative sign at half the period, l/c.

In order to calculate the solution $y(x_0, t)$ explicitly, we can decompose the function into a Fourier series using two important properties: first, that $y(x_0, t)$ is periodic in t with periodicity $2l/c$; and secondly, that the d'Alembert function $f(\lambda)$ such that $y(x_0, t) = f(x_0 + ct) - f(-x_0 + ct)$ must be periodic with periodicity $2l$. Considering $y(x_0, t)$ for a fixed value of x_0, we can use that $y(x_0, t)$ (the zig-zag, saw-tooth pattern) is periodic with period $2l/c$ with theorem 3.3.1 to write

$$y(x_0, t) = \frac{a_0}{2} + \sum_{n=1}^{\infty} a_n \cos\left(\frac{n\pi ct}{l}\right) + b_n \sin\left(\frac{n\pi ct}{l}\right). \qquad (3.28)$$

We can choose to define $t = 0$ on the saw-tooth patterns representing the displacement at x_0 arbitrarily, and so we choose $t = 0$ such that this saw-tooth waveform becomes an odd function (figure 3.1).
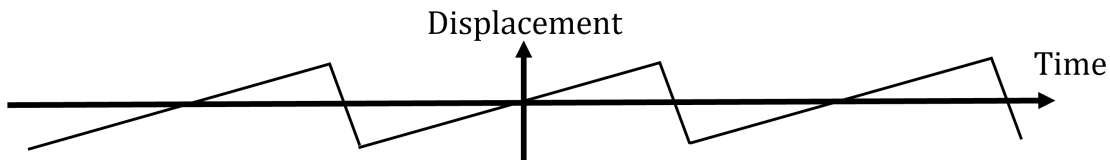

Figure 3.1: The displacement of the string at particular position with time parameterised so that the waveform is anti-symmetric about t=0, and the amplitude is zero at t=0.

This allows us to write $y(x_0, t)$ as the sum of only the odd functions in the Fourier series,

$$y(x_0, t) = \sum_{n=1}^{\infty} b_n \sin\left(\frac{n\pi ct}{l}\right). \qquad (3.29)$$

We can see from this that the spectrum of frequencies is given by the coefficients on t in the formula,

$$\boxed{\omega_n = \frac{n\pi c}{l} = \frac{n\pi}{l}\sqrt{\frac{\mu}{\rho}}} \qquad (3.30)$$

which do not depend on the value of x_0. This means that these frequencies form the spectrum of the Fourier expansion at any point on the string: if we study the motion of the string around the bridge, then we can represent the applied force of the string's oscillation on the bridge by a series of oscillations, with magnitudes given by the coefficients b_n. Indeed, we have come across a crucial point here: the spectrum of frequencies of the bowed string is the same as the spectrum of frequencies of the normal modes of the string, as the waveform on the bowed string is a superposition of the normal modes. This implies that (in our model) the bowed string is *harmonic*. Note also that the values of each Fourier coefficient b_n will depend on the position on the string x_0. In order to model the motion of the bowed string, we need to calculate b_n as a function of x_0 explicitly.

To do this, we begin by using the fact that f is periodic with period $2l$ to write f as a Fourier series in amplitude-phase form from corollary 3.3.2,

$$f(x) = \frac{c_0}{2} + \sum_{n=1}^{\infty} c_n \cos\left(\frac{n\pi x}{l} + \phi_n\right). \qquad (3.31)$$

24

Note here that the Fourier coefficient c_n for $f(x)$ must be independent of x. This is an important fact that will be used later. Next, plugging these Fourier expansions into d'Alembert's equation, $y(x_0, t) = f(x_0 + ct) - f(-x_0 + ct)$, we can relate the coefficients b_n to x_0 and c_n,

$$\sum_{n=1}^{\infty} b_n \sin\left(\frac{n\pi ct}{l}\right) = \sum_{n=1}^{\infty} c_n \cos\left(\frac{n\pi(x_0 + ct)}{l} + \phi_n\right) - \sum_{n=1}^{\infty} c_n \cos\left(\frac{n\pi(-x_0 + ct)}{l} + \phi_n\right).$$
(3.32)

As the wave equation is linear, we can solve this one component at a time:

$$
\begin{aligned}
b_n \sin\left(\frac{n\pi ct}{l}\right) &= c_n \cos\left(\frac{n\pi(x_0 + ct)}{l} + \phi_n\right) - c_n \cos\left(\frac{n\pi(-x_0 + ct)}{l} + \phi_n\right) \\
&= c_n \left(\cos\left(\frac{n\pi x_0}{l}\right) \cos\left(\frac{n\pi ct}{l} + \phi_n\right) - \sin\left(\frac{n\pi x_0}{l}\right) \sin\left(\frac{n\pi ct}{l} + \phi_n\right) \right) \\
&\quad - 2c_n \left(\cos\left(-\frac{n\pi x_0}{l}\right) \cos\left(\frac{n\pi ct}{l} + \phi_n\right) - \sin\left(-\frac{n\pi x_0}{l}\right) \sin\left(\frac{n\pi ct}{l} + \phi_n\right) \right) \\
&= -2c_n \sin\left(\frac{n\pi x_0}{l}\right) \sin\left(\frac{n\pi ct}{l} + \phi_n\right) \\
&= 2c_n \sin\left(\frac{n\pi x_0}{l}\right) \sin\left(\frac{n\pi ct}{l} + \phi_n + \pi\right) \\
&= 2c_n \sin\left(\frac{n\pi x_0}{l}\right) \sin\left(\frac{n\pi ct}{l} + \theta_n\right)
\end{aligned}
$$
(3.33)

where we have reset the phase using $\sin(\theta + \pi) = -\sin(\theta)$, and substituted $\theta_n = \phi_n + \pi$. In fact, given that we need this equation to be an identity between functions of t, we can set $\theta_n = 0$. For this identity to then hold for any value of t, we must have

$$b_n = 2c_n \sin\left(\frac{n\pi x_0}{l}\right).$$
(3.34)

We can model Helmholtz's saw-tooth pattern for $y(x_0, t)$ explicitly by writing it explicitly as a triangular waveform,

$$y(x_0, t) = \begin{cases} A\frac{t}{\alpha} & -\alpha \le x \le \alpha \\ A\frac{l-ct}{l-c\alpha} & a \le x \le \frac{2l}{c} - \alpha \end{cases}$$
(3.35)

where $\alpha \in \mathbb{R}$ is a number that depends on x_0, and determines how long the leading edge of the triangular waveform lasts at the position x_0 along the string. The quantity A also depends on x_0, and represents the maximum amplitude of the oscillation at that point - writing A as a function of x_0 will define the parabola shown in figure 1.5 [3]. We can then calculate the Fourier coefficients b_n for the function $y(x_0, t)$, which has periodicity $2l/c$ using the method given in lemma 3.3.3,

$$b_n = \frac{c}{l} \int_0^{2l/c} \sin\left(\frac{n\pi ct}{l}\right) f(t) dt,$$
(3.36)

giving

25

$$b_n = \frac{c}{l} \int_{-\alpha}^{\alpha} A\frac{t}{\alpha} \sin\left(\frac{n\pi ct}{l}\right) dt + \frac{c}{l} \int_{\alpha}^{\frac{2l}{c}-\alpha} A\frac{t-ct}{l-c\alpha} \sin\left(\frac{n\pi ct}{l}\right) dt$$

$$= \frac{2Al^2}{n^2\pi^2 c\alpha(l-c\alpha)} \sin\left(\frac{n\pi c\alpha}{l}\right),$$

(3.37)

so,

$$c_n = \frac{Al^2}{n^2\pi^2 c\alpha(l-c\alpha)} \frac{\sin(n\pi c\alpha/l)}{\sin(n\pi x_0/l)}.$$

(3.38)

As stated above, the values of c_n can't depend on the value of x_0 which we choose, and therefore the only way this can work is if the two sine terms in this ratio are equal; that is if

$$\frac{\pi c\alpha}{l} = \frac{\pi x_0}{l},$$

(3.39)

or

$$c\alpha = x_0.$$

(3.40)

If we measure the vibration at x_0 then the proportion $\alpha/(l/c)$ of the cycle spent in the trailing part of the triangular wave is equal to x_0/l. In particular, if we measure at the bowing point, we obtain the following principle, as stated in Benson's *"Music: A Mathematical Offering"* [3]:

> *"The proportion of the cycle for which the bow slips on the string is the same as the proportion of the string between the bow and the bridge."*

We stated above that A depends on x_0. As we know that c_n cannot depend on x_0, the term $A/c\alpha(l-c\alpha) = A/x_0(l-x_0)$ in equation 3.38 for c_n must be independent of x_0. If we write K for this quantity, we obtain a formula for the maximum amplitude in terms of position along the string x_0,

$$A = Kx_0(l-x_0).$$

(3.41)

We can see from this formula that $A(x_0)$ *is quadratic with respect to* x_0, which explains the parabolic amplitude envelope for the oscillation of the bowed string (figure 1.5).

Combining this gives an equation for the displacement $y(x_0, t)$ written directly in terms of x_0 and t.

$$\boxed{y(x_0, t) = \sum_{n=1}^{\infty} \frac{2Kl^2}{n^2\pi^2} \sin\left(\frac{n\pi x_0}{l}\right) \sin\left(\frac{n\pi ct}{l}\right)}$$

(3.42)

Chapter 4

Vibrations of Thin Plates

In order to model the modes of vibration of the violin base plate, we must first derive an equation that describes the vibrations of a thin elastic plate. Using the Lagrangian from linear elasticity, we derive the *Kirchoff-Love equation*, a particular form of biharmonic equation. We then derive boundary conditions for the vibrations of a free square plate, and solve for the modes of vibration in order to test our theory.

This chapter largely reproduces the results given in Stephen Timoshenko's *"Theory of Plates and Shells"* [13] a 2009 paper by S. V. Bosakov [18].

4.1 Action for the thin plate

To derive the differential equation that describes the vibrational motion for a thin plate, we begin by recalling the action for a general elastic deformation $\mathbf{u}$ in a domain $D \in \mathbb{R}^3$,

$$S = \int_0^T dt \frac{1}{2} \int_D \left(\rho \left(\frac{\partial u_k}{\partial t} \right)^2 - \lambda \left(\frac{\partial u_k}{\partial x_k} \right)^2 - \frac{\mu}{2} \left(\frac{\partial u_i}{\partial x_j} + \frac{\partial u_j}{\partial x_i} \right)^2 \right) dV. \tag{4.1}$$

where ρ is the density of the plate and λ, μ are the Lame parameters. We consider the thin plate to be oriented so that the plane $x_3 = 0 \; (= z)$ lies within the plate; that is, the x_3 (or z) axis points normal to the surface of the plate. Furthermore, if we imagine an infinitely thin membrane, then the stress in the x_3 (z) direction must be zero as the plate has no thickness. This assumption is extrapolated to the case of the thin plate (assuming that the thickness of the plate is tiny compared to the size of the plate) to say that within the inside of the plate $T_{i3} = 0$. We have the relation between T and $\mathbf{u}$

$$T_{ij} = \lambda \frac{\partial u_k}{\partial x_k} \delta_{ij} + \mu \left(\frac{\partial u_i}{\partial x_j} + \frac{\partial u_j}{\partial x_i} \right), \tag{4.2}$$

so

$$T_{i3} = \lambda \frac{\partial u_k}{\partial x_k} \delta_{i3} + \mu \left(\frac{\partial u_i}{\partial x_3} + \frac{\partial u_3}{\partial x_i} \right) = 0. \tag{4.3}$$

This gives the equations

$$\frac{\partial u_3}{\partial x_3} = -\frac{\lambda}{\lambda + 2\mu} \left(\frac{\partial u_1}{\partial x_1} + \frac{\partial u_2}{\partial x_2} \right), \tag{4.4}$$

$$\frac{\partial u_1}{\partial x_3} = -\frac{\partial u_3}{\partial x_1}, \tag{4.5}$$

$$\frac{\partial u_2}{\partial x_3} = -\frac{\partial u_3}{\partial x_2}. \tag{4.6}$$

Now, we set $v(x_1, x_2) = u_3(x_3 = 0)$, allowing us to write

$$\frac{\partial u_3}{\partial x_3} = -\frac{\partial v}{\partial x_1}, \qquad \frac{\partial u_2}{\partial x_3} = -\frac{\partial v}{\partial x_1}, \tag{4.7}$$

which can be integrated to give

$$u_1 = -x_3 \frac{\partial v}{\partial x_1}, \qquad u_2 = -x_3 \frac{\partial v}{\partial x_1}. \tag{4.8}$$

where the constants of integration were chosen so that $u_1(x_3 = 0) = u_2(x_3 = 0) = 0$. This now gives us

$$\frac{\partial u_3}{\partial x_3} = \frac{\lambda}{\lambda + 2\mu} x_3 \left(\frac{\partial^2 v}{\partial x_1^2} + \frac{\partial^2 v}{\partial x_2^2} \right). \tag{4.9}$$

As we can now express every $\frac{\partial u_i}{\partial u_j}$ as a function of v, we can write the action for a plate of thickness H as a function of v,

$$S(v) = \int_0^T dt \frac{1}{2} \int_{-\frac{H}{2}}^{\frac{H}{2}} dx_3 \int_{Plate} \left[\rho \left(\left(\frac{\partial u_1}{\partial t}\right)^2 + \left(\frac{\partial u_2}{\partial t}\right)^2 + \left(\frac{\partial u_3}{\partial t}\right)^2 \right) - \lambda \left(\frac{\partial u_1}{\partial x_1} + \frac{\partial u_2}{\partial x_2} + \frac{\partial u_3}{\partial x_3} \right)^2 \right.$$

$$-2\mu \left(\left(\frac{\partial u_1}{\partial x_1}\right)^2 + \left(\frac{\partial u_2}{\partial x_2}\right)^2 + \left(\frac{\partial u_3}{\partial x_3}\right)^2 \right) - \mu \left(\left(\frac{\partial u_1}{\partial x_2} + \frac{\partial u_2}{\partial x_1}\right)^2 + \left(\frac{\partial u_1}{\partial x_3} + \frac{\partial u_3}{\partial x_1}\right)^2 + \left(\frac{\partial u_2}{\partial x_3} + \frac{\partial u_3}{\partial x_2}\right)^2 \right) \right] dV$$

$$= \int_0^T dt \frac{1}{2} \int_{-\frac{H}{2}}^{\frac{H}{2}} dx_3 \int_{Plate} \left[\rho \left(\left(\frac{\partial v}{\partial t}\right)^2 + x_3^2 \left(\frac{\partial^2 v}{\partial t \partial x_1}\right)^2 + x_3^2 \left(\frac{\partial^2 v}{\partial t \partial x_2}\right)^2 \right) \right.$$

$$- \lambda x_3^2 \left(-\frac{\partial^2 v}{\partial x_1^2} - \frac{\partial^2 v}{\partial x_2^2} + \frac{\lambda}{\lambda + 2\mu} \left(\frac{\partial^2 v}{\partial x_1^2} + \frac{\partial^2 v}{\partial x_2^2} \right) \right)^2$$

$$- 2\mu x_3^2 \left(\left(\frac{\partial^2 v}{\partial x_1^2}\right)^2 + \left(\frac{\partial^2 v}{\partial x_2^2}\right)^2 + \left(\frac{\lambda}{\lambda + 2\mu} \left(\frac{\partial^2 v}{\partial x_1^2} + \frac{\partial^2 v}{\partial x_2^2} \right) \right)^2 \right) - 4\mu x_3^2 \left(\frac{\partial^2 v}{\partial x_1 \partial x_2} \right)^2 \right] dx_1 dx_2$$

$$= \int_0^T dt \frac{H}{2} \int_{Plate} \left[\rho \left(\frac{\partial v}{\partial t}\right)^2 + \frac{H^2}{2} \left(\rho \left(\frac{\partial^2 v}{\partial t \partial x_1}\right)^2 + \rho \left(\frac{\partial^2 v}{\partial t \partial x_2}\right)^2 - \frac{4\lambda \mu^2}{(\lambda + 2\mu)^2} \left(\frac{\partial^2 v}{\partial x_1^2} + \frac{\partial^2 v}{\partial x_2^2} \right)^2 \right. \right.$$

$$\left. -4\mu \frac{(\lambda + \mu)^2 + \mu^2}{(\lambda + 2\mu)^2} \left(\left(\frac{\partial^2 v}{\partial x_1^2}\right)^2 + \left(\frac{\partial^2 v}{\partial x_2^2}\right)^2 \right) - \frac{4\mu \lambda^2}{(\lambda + 2\mu)^2} \left(\frac{\partial^2 v}{\partial x_1^2} \frac{\partial^2 v}{\partial x_2^2} \right) - 4\mu \left(\frac{\partial^2 v}{\partial x_1 \partial x_2} \right)^2 \right) \right] dx_1 dx_2$$

$$= \int_0^T dt \frac{H}{2} \int_{Plate} \left[\rho \left(\frac{\partial v}{\partial t}\right)^2 + \frac{H^2}{2} \left(\rho \left(\frac{\partial^2 v}{\partial t \partial x_1}\right)^2 + \rho \left(\frac{\partial^2 v}{\partial t \partial x_2}\right)^2 \right. \right.$$

$$\left. \left. - 4\mu \frac{\lambda^2 + 3\mu\lambda + 2\mu^2}{(\lambda + 2\mu)^2} \left(\frac{\partial^2 v}{\partial x_1^2} + \frac{\partial^2 v}{\partial x_2^2} \right)^2 - 4\mu \left(\left(\frac{\partial^2 v}{\partial x_1 \partial x_2}\right)^2 - \frac{\partial^2 v}{\partial x_1^2} \frac{\partial^2 v}{\partial x_2^2} \right) \right) \right] dx_1 dx_2 \tag{4.10}$$

We can simplify this further by rewriting the coefficients using the Young's Modulus E_Y and the Poisson ratio ν, which are related to the Lame parameters by (check Landau and Lifshitz)

$$\mu = \frac{E_Y}{2(1 + \nu)}, \qquad \lambda = \frac{E_Y}{(1 + \nu)(1 - 2\nu)}. \tag{4.11}$$

We can now write down the action for the thin plate (exchanging x_1 for x, x_2 for y),

$$
\begin{aligned}
S(v) = \int_0^T dt \frac{H}{2} \int_{Plate} &\left[\rho \left(\frac{\partial v}{\partial t} \right)^2 + \frac{H^2}{2} \left(\rho \left(\frac{\partial^2 v}{\partial t \partial x} \right)^2 + \rho \left(\frac{\partial^2 v}{\partial t \partial y} \right)^2 \right. \right. \\
&\left. \left. - \frac{E_Y}{(1-\nu^2)} \left\{ \left(\frac{\partial^2 v}{\partial x^2} + \frac{\partial^2 v}{\partial y^2} \right)^2 + 2(1-\nu) \left(\left(\frac{\partial^2 v}{\partial x \partial y} \right)^2 - \frac{\partial^2 v}{\partial x^2} \frac{\partial^2 v}{\partial y^2} \right) \right\} \right) \right] dx dy. \quad (4.12)
\end{aligned}
$$

4.2 The Kirchoff-Love equation

From this action, we can derive an equation of motion describing the vibrations of the thin square plate. Treating the integrand of the action integral as a Lagrange density for a classical field $v(x,y)$, that is

$$
\begin{aligned}
\mathcal{L} = \frac{H}{2} &\left[\rho \left(\frac{\partial v}{\partial t} \right)^2 + \frac{H^2}{12} \left(\rho \left(\frac{\partial^2 v}{\partial t \partial x} \right)^2 + \rho \left(\frac{\partial^2 v}{\partial t \partial y} \right)^2 \right. \right. \\
&\left. \left. - \frac{E_Y}{(1-\nu^2)} \left\{ \left(\frac{\partial^2 v}{\partial x^2} + \frac{\partial^2 v}{\partial y^2} \right)^2 + 2(1-\nu) \left(\left(\frac{\partial^2 v}{\partial x \partial y} \right)^2 - \frac{\partial^2 v}{\partial x^2} \frac{\partial^2 v}{\partial y^2} \right) \right\} \right) \right],
\end{aligned} \quad (4.13)
$$

we can apply the Euler-Lagrange equation for a classical field in order to derive the equation of motion. Our Lagrange density is dependent on $\frac{\partial v}{\partial t}$, $\frac{\partial^2 v}{\partial t \partial x}$, $\frac{\partial^2 v}{\partial t \partial y}$, $\frac{\partial^2 v}{\partial x^2}$, $\frac{\partial^2 v}{\partial y^2}$ and $\frac{\partial^2 v}{\partial x \partial y}$, and so the form of the Euler-Lagrange equation that we use [19] is the rather obtuse looking

$$
\frac{\partial \mathcal{L}}{\partial v} - \frac{\partial}{\partial t} \frac{\partial \mathcal{L}}{\partial \frac{\partial v}{\partial t}} + \frac{\partial^2}{\partial t \partial x} \frac{\partial \mathcal{L}}{\partial \frac{\partial^2 v}{\partial t \partial x}} + \frac{\partial^2}{\partial t \partial y} \frac{\partial \mathcal{L}}{\partial \frac{\partial^2 v}{\partial t \partial y}} + \frac{\partial^2}{\partial x^2} \frac{\partial \mathcal{L}}{\partial \frac{\partial^2 v}{\partial x^2}} + \frac{\partial^2}{\partial y^2} \frac{\partial \mathcal{L}}{\partial \frac{\partial^2 v}{\partial y^2}} + \frac{\partial^2}{\partial x \partial y} \frac{\partial \mathcal{L}}{\partial \frac{\partial^2 v}{\partial x \partial y}} = 0. \quad (4.14)
$$

Application of this Euler-Lagrange equation yields the equation of motion

$$
-2\rho H \frac{\partial^2 v}{\partial t^2} + \frac{2\rho H^3}{12} \left(\frac{\partial^4 v}{\partial t^2 \partial x^2} + \frac{\partial^4 v}{\partial t^2 \partial y^2} \right) = \frac{2H^3 E_Y}{12(1-\nu^2)} \left(\frac{\partial^4 v}{\partial x^4} + 2\frac{\partial^4 v}{\partial x^2 \partial y^2} + \frac{\partial^4 v}{\partial y^4} \right). \quad (4.15)
$$

The term in brackets on the left-hand side can be written as

$$
\frac{\partial^4 v}{\partial t^2 \partial x^2} + \frac{\partial^4 v}{\partial t^2 \partial y^2} = \nabla^2 a. \quad (4.16)
$$

where a is the acceleration of the plate in the z direction at a position (x,y). For low (i.e. audible) frequencies of vibration, acceleration of the plate must not show a large variation for small spacial variations, so we can say

$$
\frac{\partial^4 v}{\partial t^2 \partial x^2} + \frac{\partial^4 v}{\partial t^2 \partial y^2} = \nabla^2 a \approx 0. \quad (4.17)
$$

Setting $H = 2h$ this gives the Kirchoff-Love equation for the vibrations of a thin plate [13],

$$
\boxed{-2\rho h \frac{\partial^2 v}{\partial t^2} = D\nabla^2 \nabla^2 v} \quad (4.18)
$$

where D is the "flexural rigidity" [15],

29

$$D = \frac{2h^3 E_Y}{3(1 - \nu^2)}. \tag{4.19}$$

In order find solutions to the Kirchoff-Love equation, we use the ansatz

$$v = \sin(\omega t)\Big[(Ae^{kx} + Be^{-kx})(Ce^{qy} + De^{-qy}) + (ae^{ikx} + be^{-ikx})(ce^{iqy} + d^{-iqy})\Big], \quad (4.20)$$

which can be written more compactly as $v = \sin(\omega t)W(x, y)$. Inserting this ansatz into the Kirchoff-Love equation allows us to derive the relation between the angular frequency ω and the wavenumbers k and q.

$$D\Big(k^2 + q^2\Big)^2 = \rho h \omega^2 \tag{4.21}$$

4.3 Boundary conditions for the free rectangular plate

Using Hamilton's *principle of least action*, we know that

$$\lim_{\delta v \to 0} \frac{S(v + \delta v) - S(v)}{\delta v} = 0, \tag{4.22}$$

and so to first order in δv we should have

$$\delta S = S(v + \delta v) - S(v) = 0. \tag{4.23}$$

Expanding out the variation in the action to first order in δ gives the integral

$$
\begin{aligned}
\delta S = \int_0^T dt \frac{H}{2} \int_{Plate} \Bigg[& 2\rho \frac{\partial v}{\partial t} \frac{\partial \delta v}{\partial t} + \frac{2H^2 \rho}{12}\left(\frac{\partial^2 v}{\partial t \partial x} \frac{\partial^2 \delta v}{\partial t \partial x} + \frac{\partial^2 v}{\partial t \partial y} \frac{\partial^2 \delta v}{\partial t \partial y} \right) \\
& - \frac{2H^2 E_Y}{12(1 - \nu^2)}\left(\frac{\partial^2 v}{\partial x^2} \frac{\partial^2 \delta v}{\partial x^2} + \frac{\partial^2 v}{\partial y^2} \frac{\partial^2 \delta v}{\partial x^2} + \frac{\partial^2 v}{\partial x^2} \frac{\partial^2 \delta v}{\partial y^2} + \frac{\partial^2 v}{\partial y^2} \frac{\partial^2 \delta v}{\partial y^2} \right) \\
& - \frac{2H^2 E_Y (1 - \nu)}{12(1 - \nu^2)}\left(\frac{\partial^2 v}{\partial x^2} \frac{\partial^2 \delta v}{\partial y^2} - 2\frac{\partial^2 v}{\partial x \partial y} \frac{\partial^2 \delta v}{\partial x \partial y} + \frac{\partial^2 v}{\partial y^2} \frac{\partial^2 \delta v}{\partial x^2} \right) \Bigg] = 0
\end{aligned}
\tag{4.24}
$$

Following a similar argument to the previous section, we can say that for audible frequencies,

$$\frac{\partial^2 v}{\partial t \partial x} \frac{\partial^2 \delta v}{\partial t \partial x} + \frac{\partial^2 v}{\partial t \partial y} \frac{\partial^2 \delta v}{\partial t \partial y} \approx 0 \tag{4.25}$$

Using integration by parts, the integral can be expanded into two separate integrals, one of which represents the conditions at the boundary, and the other contains the equation of motion that we derived previously. We consider the case of a rectangular plate defined by $x \in [-a, a]$, $y \in [-b, b]$. The part of the integral containing the boundary conditions becomes

$$2\rho\left[\int_{Plate}\frac{\partial v}{\partial t}\delta v\,dxdy\right]_0^T - \frac{2H^2E_Y}{12(1-\nu^2)}\left(\left[\int_0^T\int_{-b}^b\frac{\partial^2 v}{\partial x^2}\frac{\partial \delta v}{\partial x}dydt\right]_{x=-a}^{x=a} - \left[\int_0^T\int_{-b}^b\frac{\partial^3 v}{\partial x^3}\delta v\,dydt\right]_{x=-a}^{x=a}\right.$$

$$\left[\int_0^T\int_{-b}^b\frac{\partial^2 v}{\partial y^2}\frac{\partial \delta v}{\partial x}dydt\right]_{x=-a}^{x=a} - \left[\int_0^T\int_{-b}^b\frac{\partial^3 v}{\partial x\partial y^2}\delta v\,dydt\right]_{x=-a}^{x=a} + \left[\int_0^T\int_{-a}^a\frac{\partial^2 v}{\partial x^2}\frac{\partial \delta v}{\partial y}dxdt\right]_{y=-b}^{y=b}$$

$$-\left[\int_0^T\int_{-a}^a\frac{\partial^3 v}{\partial x^2\partial y}\delta v\,dxdt\right]_{y=-b}^{y=b} + \left[\int_0^T\int_{-a}^a\frac{\partial^2 v}{\partial y^2}\frac{\partial \delta v}{\partial y}dxdt\right]_{y=-b}^{y=b} - \left[\int_0^T\int_{-a}^a\frac{\partial^3 v}{\partial y^3}\delta v\,dxdt\right]_{y=-b}^{y=b}\right)$$

$$-\frac{2H^2E_Y(1-\nu)}{12(1-\nu^2)}\left(\left[\int_0^T\int_{-a}^a\frac{\partial^2 v}{\partial x^2}\frac{\partial \delta v}{\partial y}dxdt\right]_{y=-b}^{y=b} - \left[\int_0^T\int_{-b}^b\frac{\partial^2 v}{\partial x\partial y}\frac{\partial \delta v}{\partial y}dydt\right]_{x=-a}^{x=a}\right.$$

$$\left.-\left[\int_0^T\int_{-a}^a\frac{\partial^2 v}{\partial x\partial y}\frac{\partial \delta v}{\partial x}dxdt\right]_{y=-b}^{y=b} + \left[\int_0^T\int_{-b}^b\frac{\partial^2 v}{\partial y^2}\frac{\partial \delta v}{\partial x}dydt\right]_{x=-a}^{x=a}\right) = 0. \quad (4.26)$$

Two of the boundary integrals in the last bracket here can be further transformed by integration by parts. We have

$$\left[\int_0^T\int_{-b}^b\frac{\partial^2 v}{\partial x\partial y}\frac{\partial \delta v}{\partial y}dydt\right]_{x=-a}^{x=a} = \left[\int_0^T\frac{\partial^2 v}{\partial x\partial y}\delta v\,dt\right]_{\substack{x=a,x=-a,\\y=b,y=-b}} - \left[\int_0^T\int_{-b}^b\frac{\partial^3 v}{\partial x\partial y^2}\delta v\,dydt\right]_{x=-a}^{x=a},$$

$$(4.27)$$

and

$$\left[\int_0^T\int_{-a}^a\frac{\partial^2 v}{\partial x\partial y}\frac{\partial \delta v}{\partial x}dxdt\right]_{y=-b}^{y=b} = \left[\int_0^T\frac{\partial^2 v}{\partial x\partial y}\delta v\,dt\right]_{\substack{x=a,x=-a,\\y=b,y=-b}} - \left[\int_0^T\int_{a}^a\frac{\partial^3 v}{\partial x^2\partial y}\delta v\,dxdt\right]_{y=-b}^{y=b}.$$

$$(4.28)$$

The boundary integral equation then becomes

$$2\rho\left[\int_{Plate}\frac{\partial v}{\partial t}\delta v\,dxdy\right]_0^T - \frac{2H^2E_Y}{12(1-\nu^2)}\left(\left[\int_0^T\int_{-b}^b\left(\frac{\partial^2 v}{\partial x^2}+\nu\frac{\partial^2 v}{\partial y^2}\right)\frac{\partial \delta v}{\partial x}dydt\right]_{x=-a}^{x=a}\right.$$

$$-\left[\int_0^T\int_{-b}^b\left(\frac{\partial^3 v}{\partial x^3}+(2-\nu)\frac{\partial^3 v}{\partial x\partial y^2}\right)\delta v\,dydt\right]_{x=-a}^{x=a} + \left[\int_0^T\int_{-a}^a\left(\frac{\partial^2 v}{\partial y^2}+\nu\frac{\partial^2 v}{\partial x^2}\right)\frac{\partial \delta v}{\partial y}dxdt\right]_{y=-b}^{y=b}$$

$$\left.-\left[\int_0^T\int_{-a}^a\left(\frac{\partial^3 v}{\partial y^3}+(2-\nu)\frac{\partial^3 v}{\partial x^2\partial y}\right)\delta v\,dxdt\right]_{y=-b}^{y=b} -2(1-\nu)\left[\int_0^T\frac{\partial^2 v}{\partial x\partial y}\delta v\,dt\right]_{\substack{x=a,x=-a,\\y=b,y=-b}}\right) = 0.$$

$$(4.29)$$

This can be satisfied by imposing the following boundary conditions:

$$\frac{\partial v}{\partial t} = 0 \qquad \text{at} \qquad t=0, t=T; \qquad (4.30)$$

$$\frac{\partial^2 v}{\partial x^2} + \nu\frac{\partial^2 v}{\partial y^2} = 0 \qquad \text{at} \qquad x=a, x=-a; \qquad (4.31)$$

31

$$\frac{\partial^3 v}{\partial x^3} + (2-\nu)\frac{\partial^3 v}{\partial x \partial y^2} = 0 \qquad \text{at} \qquad x = a, x = -a; \qquad (4.32)$$

$$\frac{\partial^2 v}{\partial y^2} + \nu \frac{\partial^2 v}{\partial x^2} \qquad \text{at} \qquad y = b, y = -b; \qquad (4.33)$$

$$\frac{\partial^3 v}{\partial y^3} + (2-\nu)\frac{\partial^3 v}{\partial x^2 \partial y} \qquad \text{at} \qquad y = b, y = -b; \qquad (4.34)$$

$$\frac{\partial^2 v}{\partial x \partial y} \qquad \text{at} \qquad x = a, x = -a, \quad \text{and} \quad y = b, y = -b. \qquad (4.35)$$

From these boundary conditions, we can derive the normal modes for the vibrations of a thin rectangular plate with freely vibrating edges. We will then compare these normal modes to the results of an experiment, in order to show that the Kirchoff-Love equation is a good model for the vibrations of a thin plate.

4.4   Modes of vibration for the free rectangular plate

We insert our ansatz for the solutions to the Kirchoff-Love equation into the boundary condition for the corners of the rectangular plate (equation 4.35), to find that the solutions for the free rectangular plate must take the form of a sum of coupled trigonometric and hyperbolic functions:

$$v = \sin(\omega t)\left[K_1 \cos(kx)\cos(qy) + K_2 \cosh(kx)\cosh(qy)\right]; \qquad (4.36)$$

$$v = \sin(\omega t)\left[K_1 \sin(kx)\cos(qy) + K_2 \sinh(kx)\cosh(qy)\right]; \qquad (4.37)$$

$$v = \sin(\omega t)\left[K_1 \cos(kx)\sin(qy) + K_2 \cosh(kx)\sinh(qy)\right]; \qquad (4.38)$$

$$v = \sin(\omega t)\left[K_1 \sin(kx)\sin(qy) + K_2 \sinh(kx)\sinh(qy)\right]. \qquad (4.39)$$

The next step is to impose the edge boundary conditions in order to find the relations between k and q for each of these solutions. It can be shown that these relations are described by the roots of the transcendental equations [18]

$$\chi^\pm(\gamma) = \tan(\gamma) \pm \tanh(\gamma); \qquad \gamma = \alpha, \beta \qquad (4.40)$$

where $\alpha = ka$, $\beta = qb$. The required combination of $\chi^\pm$ for α and β depends on which of the four particular solutions we study.

The boundary conditions for the corners allow us to calculate ratios between K_1 and K_2 for each of these particular solutions. Using these ratios, we can write explicitly the four forms of particular solution for the free rectangular plate, including restrictions on k and q. For

$$v(x, y, t) = K \sin(\omega t)W(x, y) \qquad (4.41)$$

we have

$$W_1 = \cos(kx)\cos(qy) - \frac{\sin(ka)\sin(qb)}{\sinh(ka)\sinh(qb)}\cosh(kx)\cosh(qy), \quad \chi^+(ka) = 0, \chi^+(qb) = 0;$$

(4.42)

$$W_2 = \sin(kx)\cos(qy) + \frac{\cos(ka)\sin(qb)}{\sinh(ka)\cosh(qb)}\sinh(kx)\cosh(qy), \quad \chi^-(ka) = 0, \chi^+(qb) = 0;$$

(4.43)

$$W_3 = \cos(kx)\sin(qy) + \frac{\sin(ka)\cos(qb)}{\sinh(ka)\cosh(qb)}\cosh(kx)\sinh(qy), \quad \chi^+(ka) = 0, \chi^-(qb) = 0;$$

(4.44)

$$W_4 = \sin(kx)\sin(qy) - \frac{\cos(ka)\cos(qb)}{\cosh(ka)\cosh(qb)}\sinh(kx)\sinh(qy), \quad \chi^-(ka) = 0, \chi^-(qb) = 0.$$

(4.45)

If we now consider the slightly simpler case of a freely vibrating square plate, then we will be able to calculate a set of values that both k and q can take in order to satisfy $\chi^\pm(\gamma) = 0$ for $\gamma = ka, qb$. The equations $\chi^\pm(\gamma)$ must be solved numerically. This was done using the Newton-Raphson method, producing the following values the root γ (see Appendix B).

| γ	$\chi^+(\gamma)$	$\chi^-(\gamma)$
γ_0	0	0
γ_1	2.365	3.9266
γ_2	5.4978	7.0686
γ_3	8.6394	10.2102
γ_4	11.781	13.3518
γ_5	14.9221	16.4934
γ_6	18.0642	19.635
γ_7	21.2058	22.7765
γ_8	24.3473	25.9181
γ_9	27.4889	29.0597
γ_{10}	30.6305	32.2013

We will now denote the function $W(x, y)$ with constants $_{\gamma}n$, $_n$ as $W[n,_n]$. These modes for plotted using MatPlotLib, and the Chladni patterns for each mode were plotted as scatter diagrams by finding the x, y coordinates for which the amplitude of $W(x, y)$ is small (see Appendix B for code).
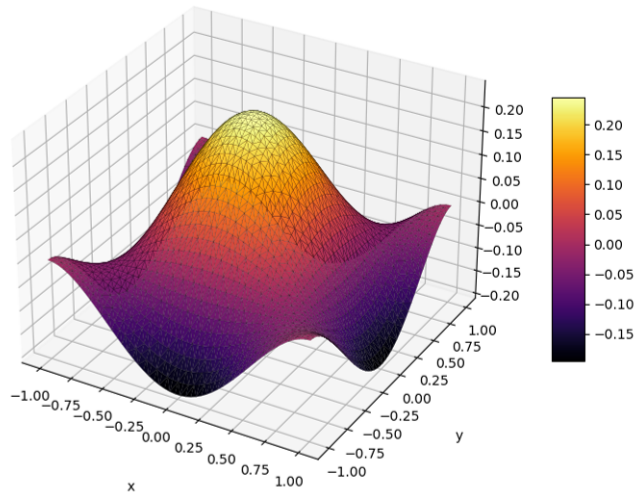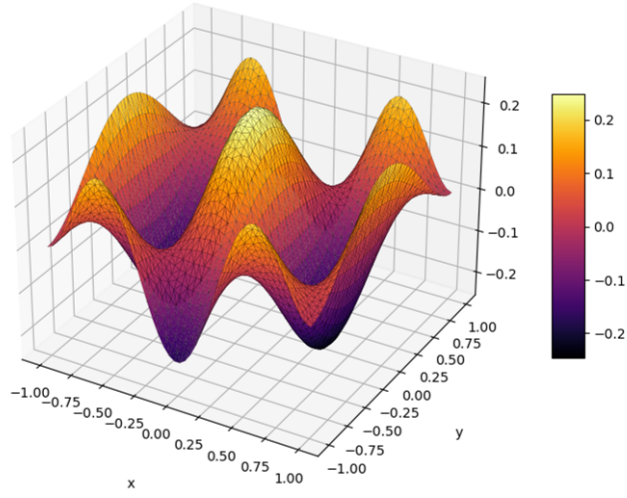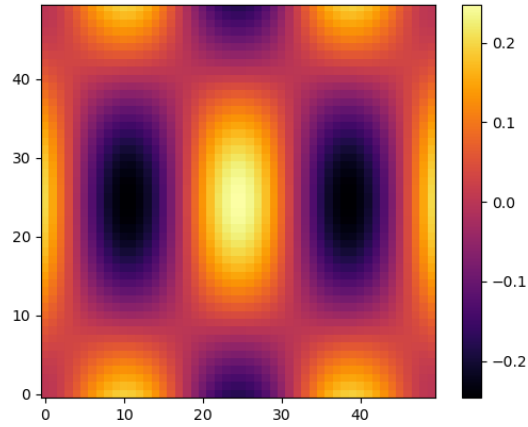
(a) 3D Plot
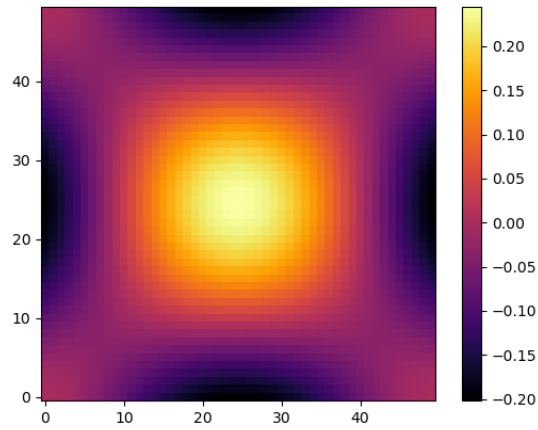
(b) Heatmap
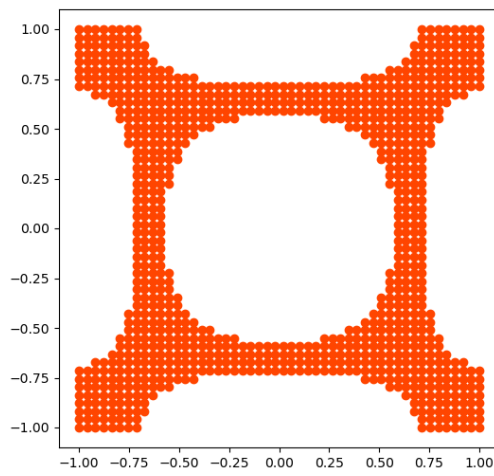
(c) Chladni Pattern

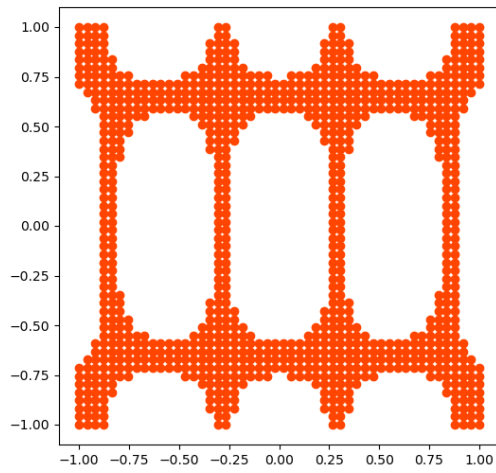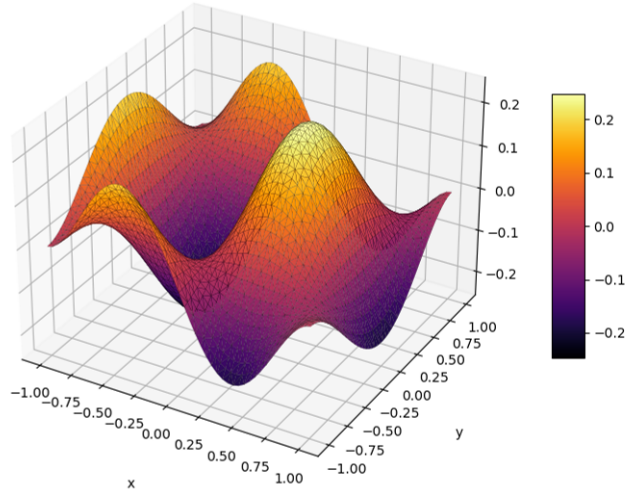Figure 4.1: The mode $W_1[k_1, q_1]$.

(a) 3D Plot

(b) Heatmap

(c) Chladni Pattern

Figure 4.2: The mode $W_1[k_2, q_1]$.

(a) 3D Plot

(b) Heatmap

(c) Chladni Pattern

Figure 4.3: The mode $W_2[k_1, q_1]$.

(a) 3D Plot

(b) Heatmap

(c) Chladni Pattern

Figure 4.4: The mode $W_3[k_1, q_1]$.

(a) 3D Plot

(b) Heatmap
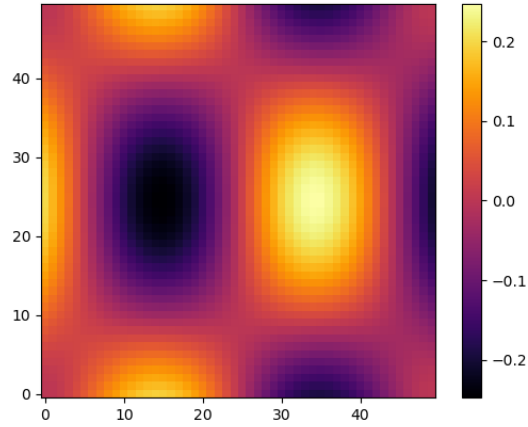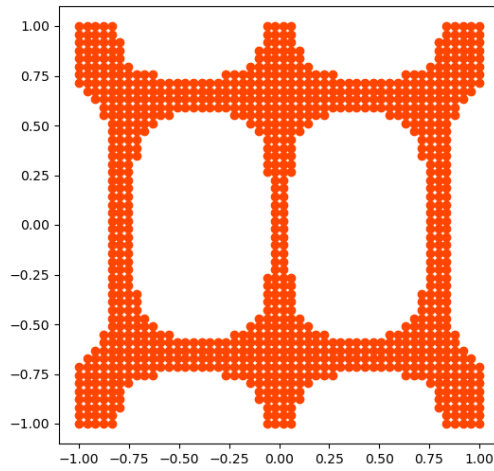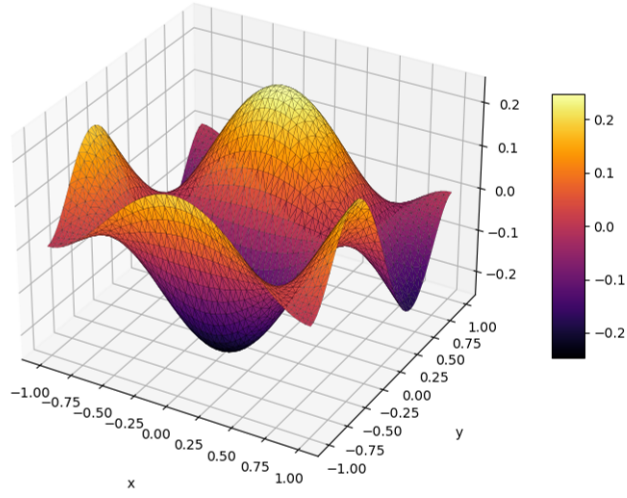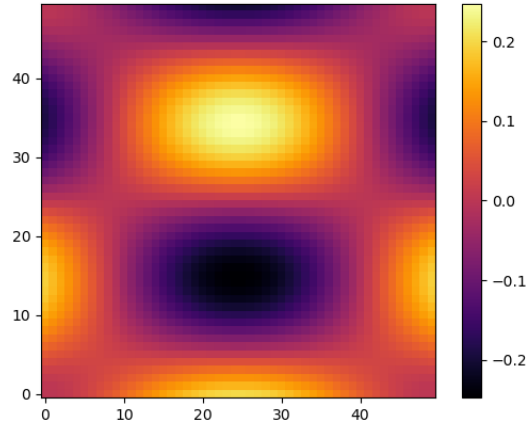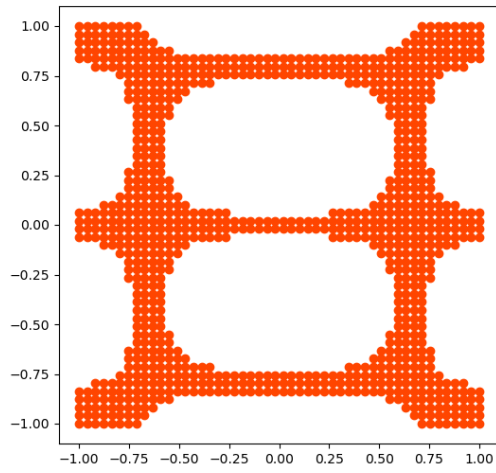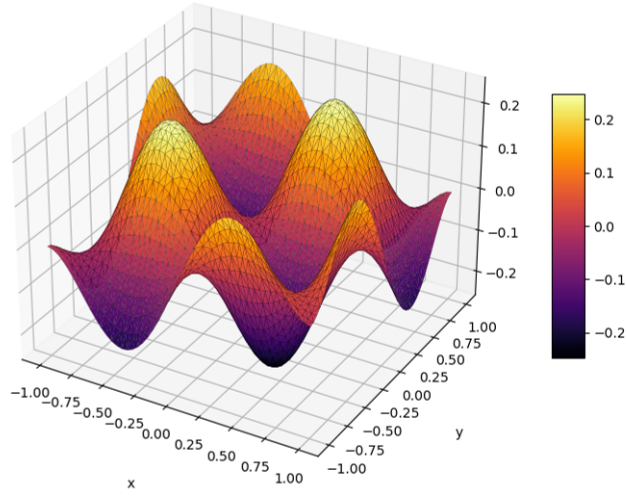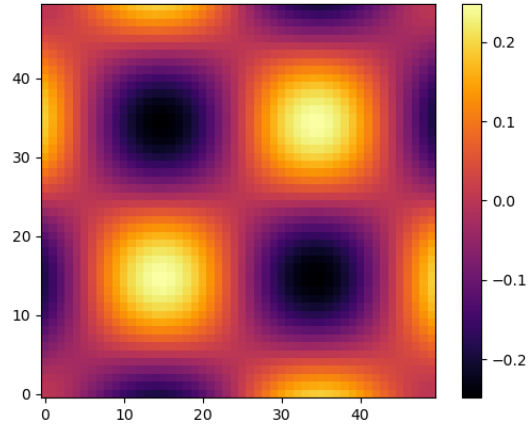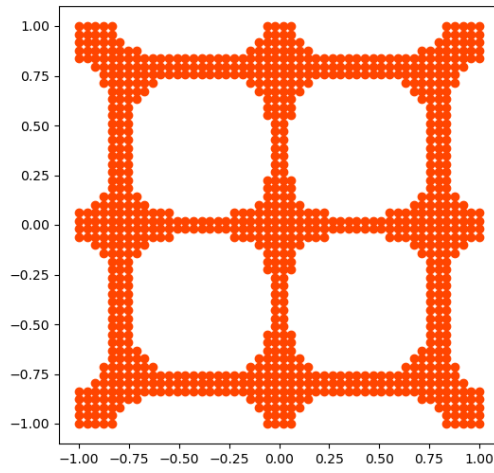

(c) Chladni Pattern

Figure 4.5: The mode $W_4[k_1, q_1]$.

4.5   Comparison with experiment

Using the values of ka and qb that we have calculated, we can plot the resulting waveforms $W(x, y)$ and compare their geometry with experimental results.

Setting $a = 1$, $b = 1$, we find that the first mode of vibration for W_1 can be found for $k = 2.365$, $q = 2.365$.

(a) 3D Plot

(b) Chladni Pattern
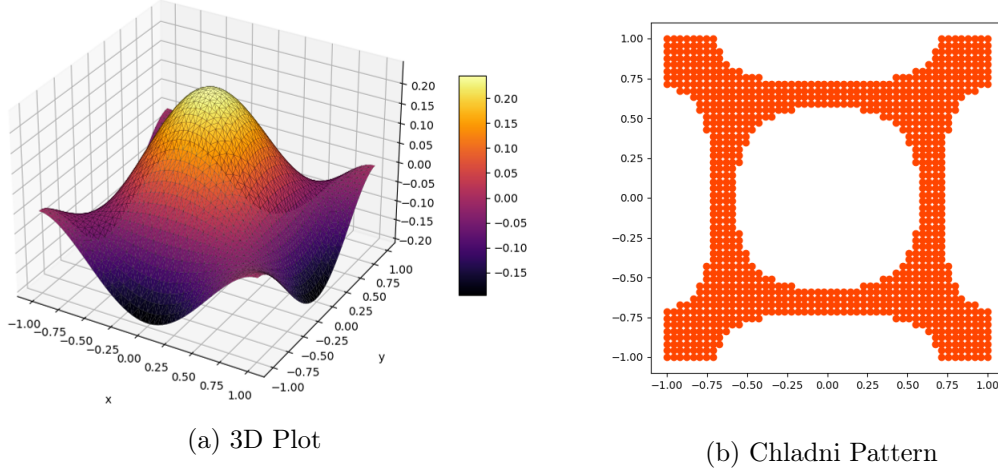
Figure 4.6: A plot of $W_1(x, y)$ for $k, q = 2.365$

In order to produce this waveform physically, a square nylon plate was used. Nylon has Young's modulus $E_Y = 2.7 \times 10^9$Pa Poisson ratio $\nu = 0.39$ [20]. The density of Nylon is $\rho = 1140$ kg / m^3 [21]. The plate measured 24 cm by 24 cm, and therefore $a = b = 0.12m$, and had a thickness $H = 3 \times 10^{-3}m$. We can calculate the values k and q for the first mode of vibration with $\alpha = \beta = 2.364$, so $k = q = \frac{2.365}{0.12}$.

We can then calculate the values of D and ω for $H = 2h$ using

$$D = \frac{E_Y H^3}{12(1 - \nu^3)}, \tag{4.46}$$

and

$$\left(k^2 + q^2\right)^2 = \frac{\rho H \omega^2}{D}. \tag{4.47}$$

The frequency of the first mode of vibration for the free square nylon plate was calculated to be 179 Hz.

A Chladni plate experiment was then conducted to identity the Chladni pattern, which should represent the lines where $W(x, y) = 0$. The the free square nylon plate was fixed in the centre to a vibration driver, powered by a frequency generator, and with the frequency generator connected to an oscilloscope to provide fine-tuning of the driving frequency. This models how the vibrations in the violin backplate are produced by the coupling of the violin body to the vibrations of the string through the sound post. At frequencies in the range of 150-160 Hz, the following Chladni pattern was found (figure 4.7).

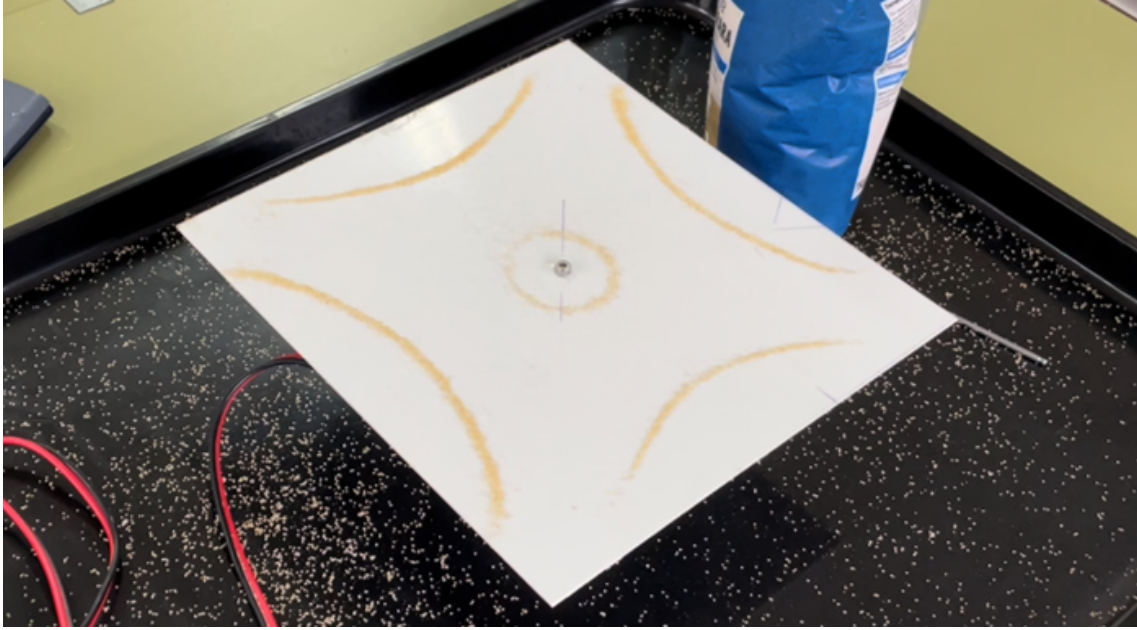Figure 4.7: The Chladni pattern found at frequency of around 150-160 Hz in my experiment.

It is clear from this photograph that the nodal lines on the Chladni plate for the mode of vibration at 150-160 Hz are a close match to the nodal lines for the waveform $W_1(x, y)$ with $k, q = 2.365$, which our model predicted should be found at 179 Hz. Notice that there is a small ring around the driving point however, and that the nodal lines for the plate in the experiment are slighter further from the centre than in our plot, in addition to the fact that there is a slight difference in the frequency that this pattern was found at. These discrepancies can be assumed to be a result of the presence of the driving force at the centre of the plate, generated by an oscillating device screwed into the plate which imposes an additional constraint on the dynamics. Indeed, if we study the next mode of vibration for W_1 which is shown in figure 4.2, then a brief calculation will show that this mode appears at a frequency of 573 Hz, which is a huge variation from the frequency that this pattern was found at in the experiment. Note that we only need to consider modes W_1 for this experiment, because these are the normal modes in which the centre of the plate is oscillating. Furthermore, the mode found in this experiment does *broadly* match the plot in figure 4.6: it has the correct degree of symmetry along the x and y axes, and has roughly the correct shape of nodal lines. From this we can infer that we have found the same mode of vibration $W_1[k_1, q_1]$, up to the influence of the driving force. It is also possible that the damping force due to air resistance plays a role in slightly offsetting the frequency and Chladni pattern for $W_1[k_1, q_1]$. The effect of damping and the driving force will be key in the next section, when we will include a driving force from the sound post in the Kirchoff-Love equation.

The accuracy of our physical prediction provides experimental evidence to justify that the Kirchoff-Love equation, along with our free boundary conditions, is a good model for the vibrations in thin, isotropic elastic plate. Given the strength of the Kirchoff-Love equation in predicting the physical modes of resonance, we will use it to model the resonant modes of vibration for the backplate of the violin, driven by the oscillations of the soundpost.

Chapter 5

Modelling the Violin Backplate

We have found that the Kirchoff-Love equation is an excellent model for the elastic vibrations in a thin isotropic plate. We will now extend the Kirchoff-Love equation to include applied forces, including and applied driving force, and solve the differential equation numerically for a flat, thin, violin-shaped plate in order to model the modes of vibration of the violin back plate when coupled to the vibrations of the strings through the sound post.

5.1   Extending the Kirchoff-Love equation

We have previously derived a differential equation which we called the *Kirchoff-Love equation*,

$$-2\rho h \frac{\partial^2 v}{\partial t} = D\nabla^2 \nabla^2 v, \qquad \text{with } D = \frac{2h^3 E_Y}{3(1-\nu^2)}. \tag{5.1}$$

This was in fact a special case of the more general equation originally derived by A. E. H. Love, in which we have neglected any applied forces. We now reintroduce these applied forces in order to re-derive the general Kirchoff-Love equation.

For a plate defined as a domain $S \in \mathcal{R}^2$, we define the applied force by some function $q(x, y)$ on S. For a vertical displacement $v(x, y)$ on S, the work done by the displacement at every point is given by the force of resistance multiplied by the displacement, that is,

$$W(t) = \int_S q(x, y, t)v(x, y, t)dxdy. \tag{5.2}$$

This work done then represents the potential energy gained by the system in the displacement. Introducing this term into the Lagrange density $\mathcal{L} = T - V$ we get an extra term

$$\mathcal{L}_{External forces} = q(x, y, t)v(x, y, t). \tag{5.3}$$

Application of the Euler-Lagrange equation for field (equation 4.14) gives the general Kirchoff-Love equation

$$\boxed{-q(x, y, t) - 2\rho h \frac{\partial^2 v}{\partial t^2} = D\left(\frac{\partial^4 v}{\partial x^4} + 2\frac{\partial^4 v}{\partial x^2 \partial y^2} + \frac{\partial^4 v}{\partial y^4}\right)} \tag{5.4}$$

where we have returned to partial derivative notation for the double Laplacian operator in preparation for solving this equation numerically.

5.2   Introducing damping

In real world systems, the oscillations of any vibrating body are effected by external forces not accounted for in the simple mechanical equations of motion, acting to damp the motion of the system. In this case, the vibrations in the violin body are damped by forces such as air resistance and forces of internal friction in the material. Damping forces such as friction typically are typically linearly proportional to the velocity of the oscillation,

$$F = -Q\frac{\partial v}{\partial t} \tag{5.5}$$

where Q is some "damping coefficient" and v is the vertical displacement of the plate. The negative sign here is an indication that the damping force acts in opposition to the motion of the body.

We can introduce this term into the Kirchoff-Love equation (equation 5.4) by writing the applied force $q(x, y, t)$ as a damping force,

$$q_{Damping}(x, y, t) = -Q\frac{\partial}{\partial t}v(x, y, t), \tag{5.6}$$

and hence the equation of motion for the damped thin elastic plate becomes

$$-2\rho h\frac{\partial^2 v}{\partial t^2} = D\left(\frac{\partial^4 v}{\partial x^4} + 2\frac{\partial^4 v}{\partial x^2 \partial y^2} + \frac{\partial^4 v}{\partial y^4}\right) - Q\frac{\partial v}{\partial t}. \tag{5.7}$$

5.3   The vibrations of the sound post

In order to account for the vibrations of the sound post in our model, we can use a very simple formula for the applied force. The sound post will oscillate over time, at an applied frequency ω and with some amplitude that we call k. For a force applied at a location $x_0, y_0 \in S$, where S is the domain of the plate, we have

$$q_{Driving}(x, y, t) = k\sin(\omega t)\delta(x - x_0)\delta(y - y_0). \tag{5.8}$$

In reality, our driving force will actually be a superposition of different oscillations, each with a different frequency and amplitude - each frequency will be one of the harmonic frequencies given by equation 3.30, with the amplitude of each of these oscillations proportional to the corresponding coefficient in the equation 3.42. However, for simplicity, we will consider a driving force with a single frequency, on the assumption that the vibrational behaviour of the violin body will be dominated by the frequency with largest amplitude.

The question remains, how do we choose the right value for the maximum amplitude k? If we consider a small material element on the plate at position x_0, y_0 (i.e. beneath the sound post) that is disconnected from the rest of the plate, then this formula describes the force (mass times acceleration) of this material element; that is the acceleration of the element satisfies the formula

$$2\rho ha = k\sin(\omega t)\delta(x - x_0)\delta(y - y_0), \tag{5.9}$$

where a is the acceleration of the element and $2\rho h$ is the mass density per unit area of the element. Integrating this gives the formula for the displacement of the element,

$$v(x_0, y_0, t) = -\frac{k}{2\rho h\omega^2}\sin(\omega t) \tag{5.10}$$

which indicates that the coefficient $k/2\rho h\omega^2$ represents the maximum amplitude of the oscillations driven by the sound post, i.e. the maximum distance that the sound post will move during an oscillation. We can then calculate the value of k for a given angular frequency ω essentially by estimation: the sound post cannot move very far during the oscillation. We can estimate the it should move some distance that is greater than the thickness of the string (as the amplitude of oscillations of the string must be greater than the thickness of the strong) but less that the thickness of the violin back plate (or else we the sound post could damage the violin structure through stretching). This would place the value of the coefficient $k/2\rho h\omega^2$ roughly in the order of 1-2mm, but the value could vary slightly outside of this depending on frequency. The coefficient k (which may be dependent on frequency) can then be calculated roughly using this. We will make the conservative estimate that the amplitude of oscillation is around 1 mm $= 1 \times 10^{-3}$m, requiring that $k = (1 \times 10^{-3} \times 2\rho h\omega^2)$.

Combining these equations for applied forces gives us an expression of the Kirchoff-Love differential equation that we can solve numerically for our violin body model.

$$-2\rho h \frac{\partial^2 v}{\partial t^2} = D\left(\frac{\partial^4 v}{\partial x^4} + 2\frac{\partial^4 v}{\partial x^2 \partial y^2} + \frac{\partial^4 v}{\partial y^4}\right) - Q\frac{\partial v}{\partial t} + k\sin(\omega t)\delta(x - x_0)\delta(y - y_0) \qquad (5.11)$$

The final development that is required for our model of the vibrations on the violin-shaped plate is the imposition of relevant boundary conditions.

5.4   The boundary conditions for the back plate

The edge of the violin plate must be fixed because it is glued in place to the body of the violin. As the edge is fixed for all time, everywhere on the boundary of the shape S, we can conclude that the boundary conditions are

$$v(x, y, t) = 0, \quad \frac{\partial v}{\partial t} = 0, \frac{\partial v}{\partial x} = 0, \frac{\partial v}{\partial y} = 0, \qquad \text{on } \partial S. \qquad (5.12)$$

The next step is to choose a shape $S \in \mathcal{R}^2$ that resembles the shape of the violin. A simple geometric shape that fits this description is the *hippopede*. A hippopede is a curve of the form

$$\left(x^2 + y^2\right)^2 = cx^2 + dy^2, \qquad \text{with} \quad c > 0, d > 0. \qquad (5.13)$$

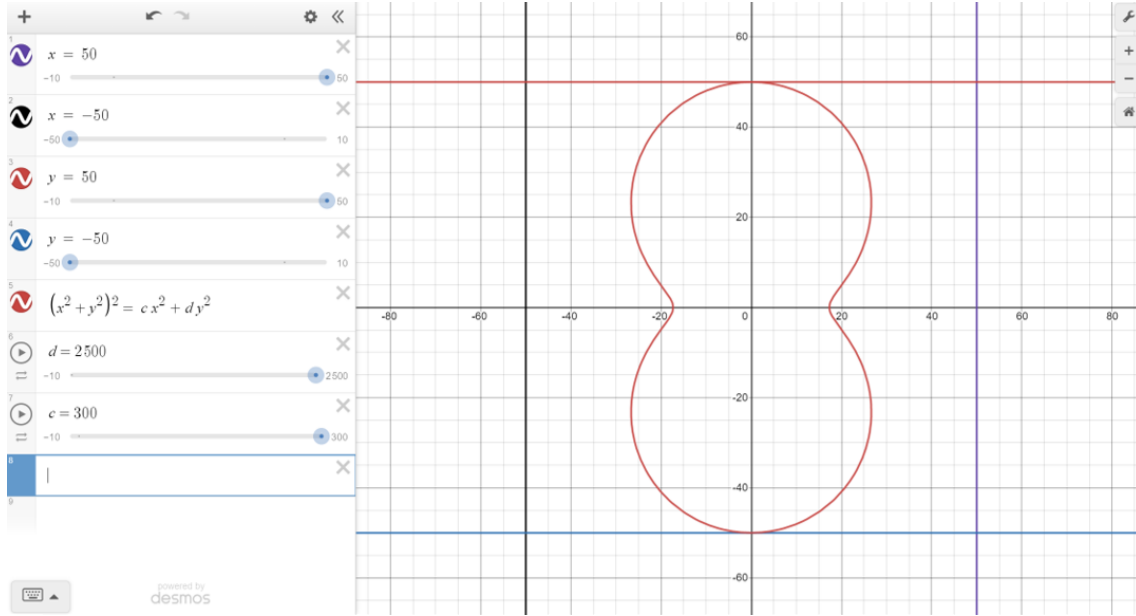A simple plot of this shape shows that it resembles the shape of the violin base plate (figure 5.1).

Figure 5.1: A plot of a hippopede, produced in Desmos. With $c = 300$, $d = 2500$, the shape has a length along the major axis of 100.

5.5 Numerical solutions for the violin back plate

Before we begin to model the violin back plate, we must find the right physical characteristics for the wood. Specifically we need to know the Young's modulus E_Y, the Poisson ratio ν, the thickness of the plate H, and the density ρ of the wood.

Contemporary violins are modelled on Italian works from the 17th and 18th centuries. In these instruments, maple wood, was chosen for the construction of the back plate. [22] For maple wood, we take $E_Y = 12600$ MPa $= 12.6 \times 10^9$ Pa, $\nu = 0.044$, and $\rho = 530$ kg/m^3. It should be noted that these values are far from accurate in all physical circumstances, as the exact measurement of the Young's modulus and Poisson ratio depends or whether then measurements were taken along or against the grain of the wood. [23] [24] The thickness of the back plate varies slightly moving further away from the centre, but typically has a value around $H = 3$ mm. [1]

The constants in the Kirchoff-Love equation for our model (equation 5.11 can be rearranged to give a simpler form with just three coefficients that could be used to find numerical solutions,

$$\frac{\partial^2 v}{\partial t^2} = -A\left(\frac{\partial^4 v}{\partial x^4} + 2\frac{\partial^4 v}{\partial x^2 \partial y^2} + \frac{\partial^4 v}{\partial y^4}\right) + B\frac{\partial v}{\partial t} - C sin(\omega t)\delta(x - x_0)\delta(y - y_0), \qquad (5.14)$$

where

$$A = \frac{D}{2\rho h}, \qquad B = \frac{Q}{2\rho h}, \qquad C = \frac{k}{2\rho h}. \qquad (5.15)$$

The next step is to calculate values for these coefficients to use to find numerical solutions. Combining the values given above implies that for the violin back plate,

$$D = \frac{2 \times (1.5 \times 10^{-3}\text{m})^3 \times 12.6 \times 10^9\text{Pa}}{3 \times (1 - 0.044^2)} = 28.4\text{kg m}^2 \text{ s}^{-2},$$

$$\longrightarrow A = \frac{28.4\text{kg m}^2 \text{ s}^{-2}}{2 \times 530\text{kg m}^{-3} \times (1.5 \times 10^{-3}\text{m})} = 17.9 \text{ m}^4 \text{ s}^{-2}. \tag{5.16}$$

Furthermore, we find from assumptions and approximations made in section 5.3 that $C = 1 \times 10^{-3}$ m $\times \omega^2$. Finally, we need to find the right value of B, which requires an appropriate value for Q.

In order to run a demonstration of a numerical solution to this equation, I had to select physical parameters that would allow the program to run in a "reasonable" length of time. This meant that I had to select parameters A,B and C with *relatively* similar orders of magnitude.

We can keep our value of around 18 for A. To find a specific value of C, we take a frequency of a similar order of magnitude to a musical note, say, 100 Hz, and from this we calculate $C = 1 \times 10^{-3} \times (2\pi \times 100)^2 \approx 400$. We can pick the damping coefficient to be smaller than these two figures (to simulate the small force of air resistance) but of a relatively similar order of magnitude. Setting $B = 1$ suits these requirements.

In order to reduce the integration time for the simulation, plate of total length 10 (metres) was used, divided up into a 100×100 grid. This is obviously not a representation of the actual size of the violin, however the code took a large amount of time to run, so some simplifications had to be made. The results of the numerical integration program are hence a proof-of-concept demonstration that this simulation *can* be used to model vibrations in a *violin shaped plate*. The boundary conditions for the differential equations were imposed by setting both v and the derivatives of v to be zero along, and outside, the hippopede shown in figure 5.1. The full code will be included in Appendix B, and therefore could be re-run on a more powerful computer to produce a real physical simulation of the violin.

The following plots are the result of the numerical integration of the Kirchoff-Love equation, including driving and damping forces. The code performs a 4th order Runge-Kutta integration of the Kirchoff-Love equation, where equation 5.14 must be split up into a system of two time-dependent differential equations in order to be integrated:

$$\frac{\partial v}{\partial t} = u, \tag{5.17}$$

$$\frac{\partial u}{\partial t} = -A \left(\frac{\partial^4 v}{\partial x^4} + 2\frac{\partial^4 v}{\partial x^2 \partial y^2} + \frac{\partial^4 v}{\partial y^4} \right) + Bu - C sin(\omega t)\delta(x - x_0)\delta(y - y_0). \tag{5.18}$$

This system of equations was then integrated for a 100×100 mesh. The time step for the integration should be at least smaller than $\frac{dx^2}{\sqrt{k}}$. The figures produced were then taken as heat maps of the value of v at each point on the mesh, at the given values of time T (figures 5.2 to 5.8).
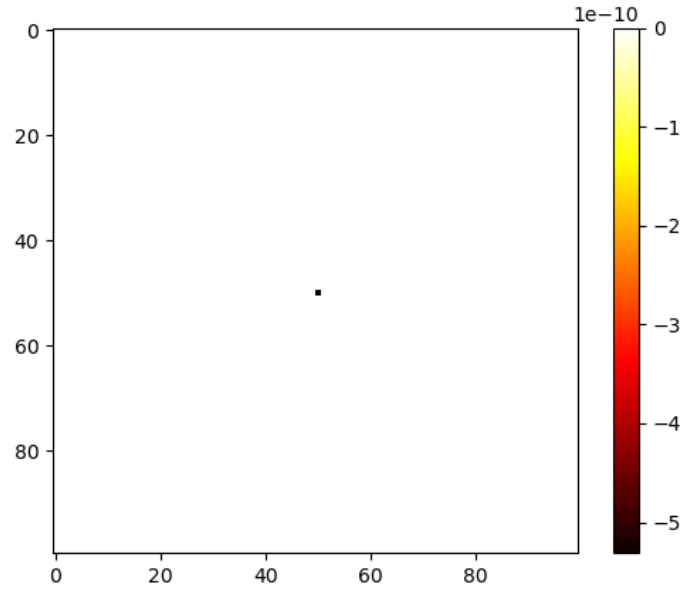
Figure 5.2: $T = 0$
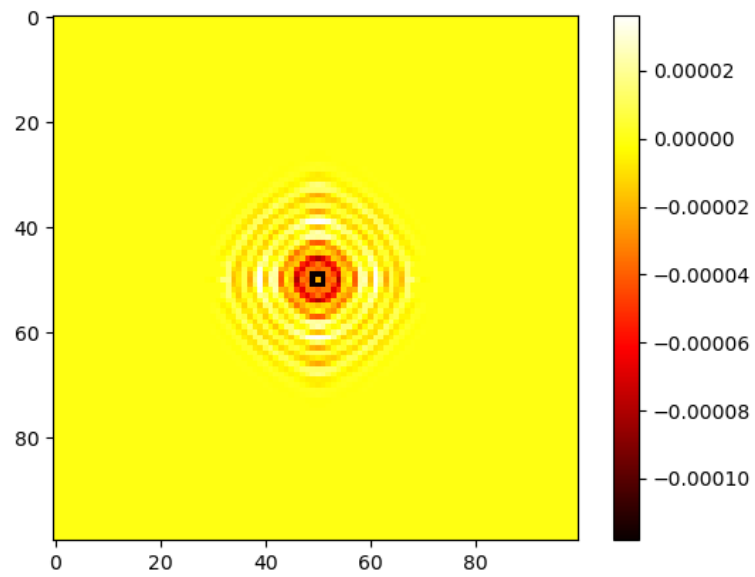
Figure 5.3: $T = 1$
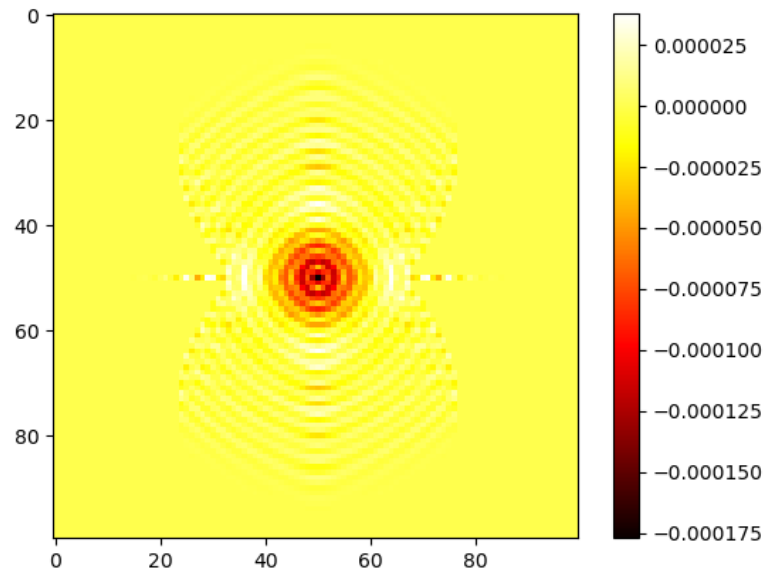
Figure 5.4: $T = 2$
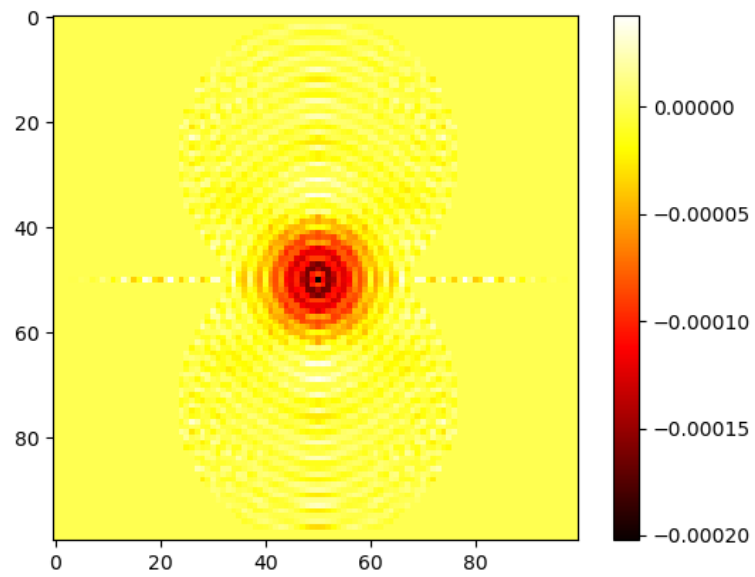
Figure 5.5: $T = 3$
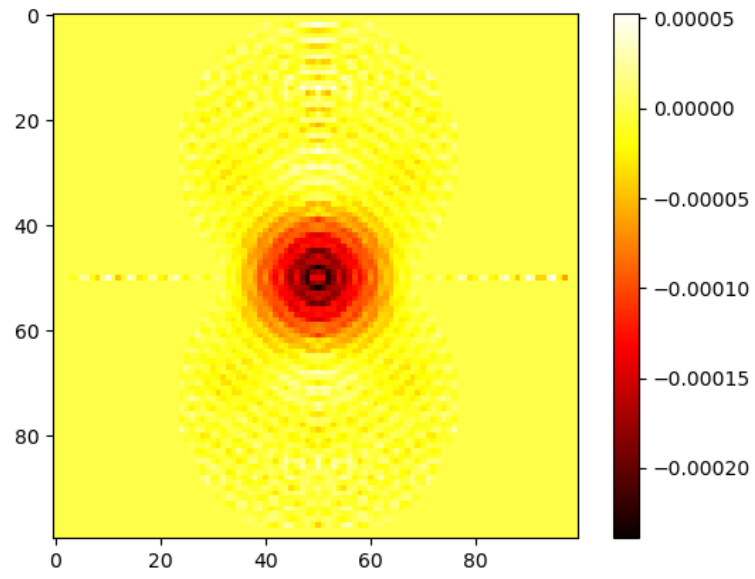
Figure 5.6: $T = 4$
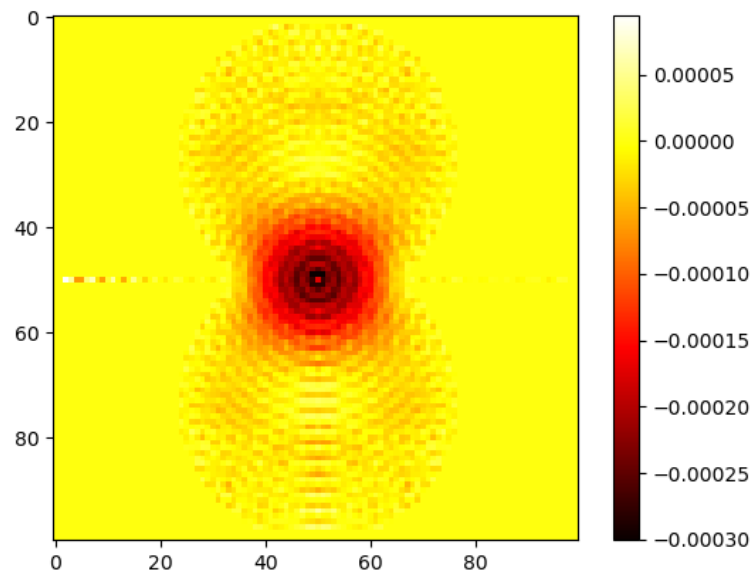
Figure 5.7: $T = 5$
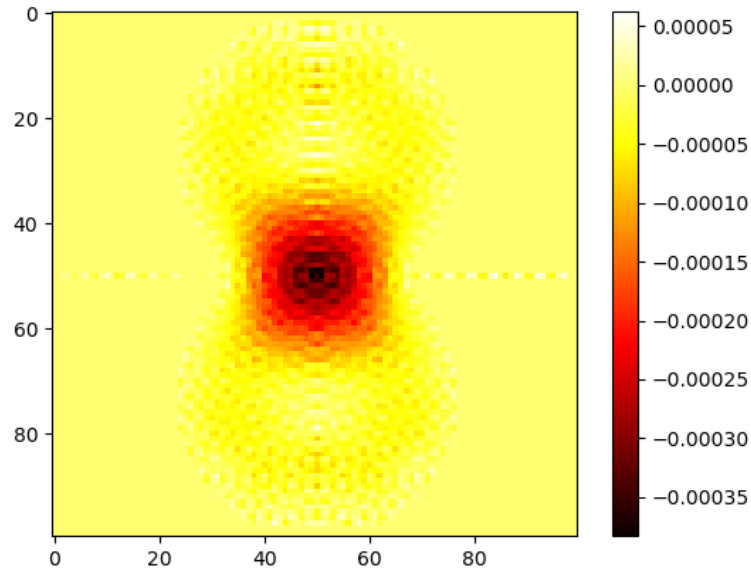
Figure 5.8: $T = 6$

We can see that figures 5.2 to 5.5 show the ripple-like motion of the vibrations propagating across the violin body from the central driving point. Then, the patterns in figures 5.6 and 5.7 appear to show the formation of something that looks like a standing wave. The figure 5.8 (and figures for later times) show the solution then blowing up - this is likely because the coefficient of the driving force was set to too large a value, and the damping set too small.

By studying the heat map shown in figure 5.7 we can construct the shape of the Chladni pattern for this mode of vibration by observing the lines where $v \approx 0$ (figure 5.9).
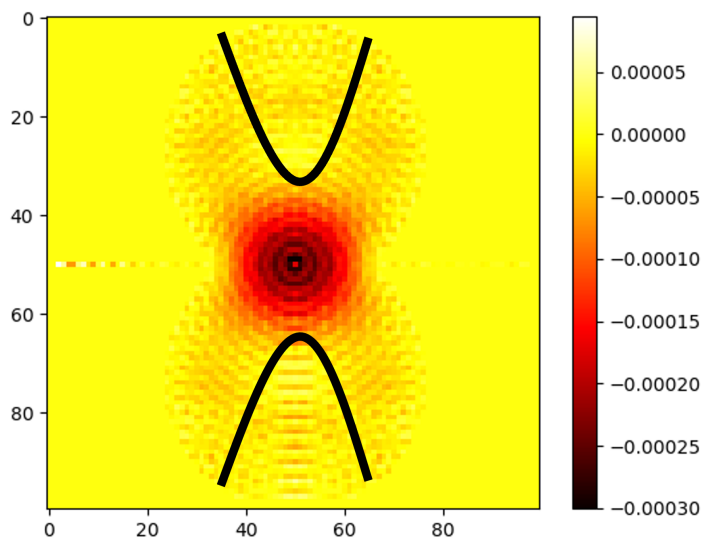
Figure 5.9: Nodal lines for the vibrations at $T = 5$, showing a Chladni pattern.

49

In fact, the nodal lines for this pattern of vibration bear a resemblance to a real mode of vibration found in the violin back plate (figure 5.10).

Figure 5.10: Chladni pattern found for a violin, which resembles the nodal lines found in our simulation.[VIII]

It should be stressed here that our simulation has *not* produced a perfect physical model for the mode of vibration shown in figure 5.10 - this is because our simulation was for a plate of a different size, and with inaccurate physical parameters that cause the solutions to blow up over a large time. However, what we have been able to demonstrate here is that our simulation does produce wave forms in a violin-shaped plate that appear to *roughly* resemble the Chladni modes of a real, physical violin back plate. This is an indication that our process for modelling the vibrations in the violin body does bear some resemblance to reality, and a more careful choice of physical parameters along with greater computing power should yield a complete physical model for the true acoustic behaviour of the violin back plate.

[VIII]https://newt.phys.unsw.edu.au/jw/chladni.html

Chapter 6

Conclusion

This project has developed a set of mathematical models to describe and explain the mechanics of the violin.

To begin with, the mathematical theory of elastic bodies was developed. By finding the relationship between stresses and strains in isotropic materials, equations for the motion and energies of elastic displacements in a material were derived. These equations are used a tool for the derivation of relevant equations of motion for a particular elastic body using the principle of least action.

Following this, the theory of elasticity was used to show that vibrations in a stretched string were described by the wave equation. This equation was solved for the bowed string using d'Alembert's and Fourier's methods, which consequently provided an explanation for the prescribed parabolic shape drawn out by the motion of the bowed string.

The equations for the elastic energies of a material, applied to the case of a thin elastic plate, were used to derive the Kirchoff-Love equation of motion for the vibrations in a thin plate. Using Hamilton's principle of least action, the boundary conditions for a freely vibrating rectangular plate were found. The Kirchoff-Love equation was then solved analytically to find the normal modes of a thin square plate, and it was demonstrated experimentally that these equations provide an accurate model for the vibrations in a thin elastic plate.

Finally, a physical model for the vibrations of the violin body was developed based on the Kirchoff-Love differential equations, to account for both the vibrations driven by the violin strings, and a force acting to damp the vibrations. With the imposition of relevant boundary conditions on a violin shaped plate, these equations were solved numerically used the 4th order Runge-Kutta method to model the elastic vibrations in the body of the violin.

The avenues for further study following the conclusion of this project are diverse. In chapter 3 it was stated that in our model, the spectrum of frequencies for the bowed violin string was harmonic. However, a more sophisticated model taking into account the full 3-dimensional structure of the string may show that the spectrum is more complicated than our simple 2-dimensional model would suggest. Indeed, in *"Vibration and Sound"*, Philip M. Morse suggests a fourth-order partial differential equation to describe the motion of a stiff string [25]. A similar equation could provide a more accurate physical model for behaviour of the bowed string, contradicting our prediction that the spectrum for the bowed string is harmonic.

Additionally, a more advanced study of the normal modes of the violin back plate could be undertaken in order to directly predict the Chladni patterns for the violin back plate, using the differential equations given in this report. Such a study is given by C. Gough in a 2015 paper for the Journal of the Acoustical Society of America [26]. Using the Comsol finite element software, Gough includes additional boundary constraints of the ribs, and bass-bar (see figure 1.3) as well as the sound post to model the vibrational modes of the violin. Gough changes the physical parameters in his model continuously, to study the effect on the modes of vibration of variations in the shape and arching of the violin. Moreover, by modelling the vibrations in the back plate of the violin only, it was not necessary for us to study the effect of the f-holes on the acoustic behaviour of the violin. Gough's paper models both the front and back plate of the violin, and hence accounts for the acoustic consequences of the f-holes.

Figure 6.1: Modes of vibration of the violin-shaped plate computed by C. Gough [26].
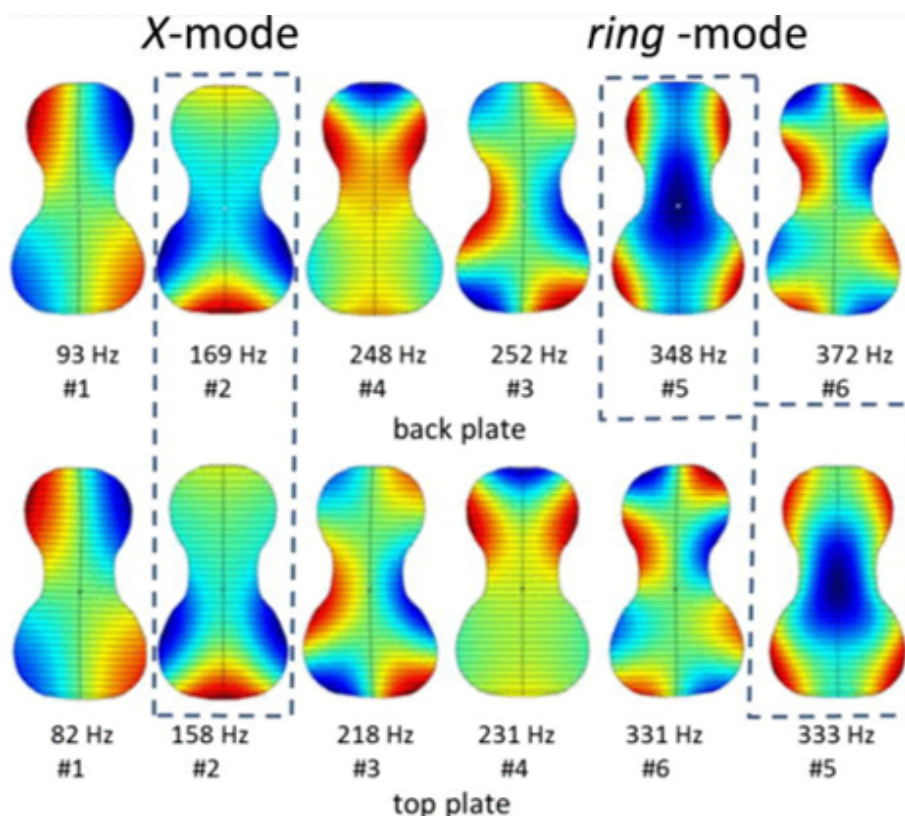
Finally, the development of the theory of linear elasticity given in chapter 2, the relations between stresses and strains, along with the equations of energy and motion, were derived for isotropic elastic materials only. In reality, the wood that makes up the body of the violin is highly anisotropic as response of the material to elastic displacements will depend on whether the elastic stresses and strains are acting along or against the grain of the wood. Chapter 11 of Timoshenko's *"Theory of Plates and Shells"* gives a differential equation for the elastic behaviour of a thin plate that takes into account anisotropy of the plate in the x and y directions [13]. An equation similar to this could be included in our model in order to account for the anisotropy of the violin body due to the grain of the wood. The solutions to such a model may provide a physical explanation for the differences in acoustic quality of different violins.

Bibliography

[1] E. Heron-Allen. *Violin-Making : As it was and is.* Ward, Lock and Co., 1885.

[2] H. Helmholtz. *On the sensations of tone as a physiological basis for the theory of music.* Longmans, Green, and Co., 1895.

[3] D. J. Benson. *Music: A Mathematical Offering.* Cambridge University Press, 2007.

[4] R. Wood. *The Physics of Music.* Meutheun Co. Ltd., 1944.

[5] G. V. B. Galilei (1638). *Dialogues concerning two new sciences.* New York Macmillan, 1914.

[6] R. Hooke. *The Diary of Robert Hooke.* Taylor Francis, 1672-1680.

[7] E. Chladni. *Discoveries in the Theory of Sound.* 1787.

[8] J. D. McLennan. *The violin: music acoustics from Baroque to Romantic.* PhD thesis, University of New South Wales, 2008.

[9] Benning Violins. Violinmaking and chladni patterns. `https://www.benningviolins.com/violinmaking-and-chladni-patterns.html`.

[10] San Diego Supercomputer Centre. Sophie Germain: Revolutionary Mathematician. `https://www.sdsc.edu/ScienceWomen/germain.html`.

[11] V. C. Petrovich. Women and the Paris Academy of Sciences. *Eighteenth-Century Studies*, 32(3), 1999.

[12] S. Germain. *Recherches sur la théorie des surfaces élastiques.* M.me v.e Courcier, 1821.

[13] S. Timoshenko and S Woinowsky-Krieger. *Theory of Plates and Shells.* McGraw-Hill Book Company, Inc., 1959.

[14] D. J. Raymond. *Introduction to Continuum Mechanics.* New Mexico Institute of Mining and Technology, 2009.

[15] L. D. Landau and E. M. Lifshitz. *Theory of Elasticity: Course of Theoretical Physics, Volume 7.* Elsevier, third edition, 1986.

[16] K. Aki and P. G. Richards. *Quantitative Seisomology.* University Science Books, 2002.

[17] P. Sutcliffe. Calculus I Lecture Notes. *University of Durham*, 2018/19.

[18] S. V. Bosakov. Eigenfrequencies and modified eigenmodes of a rectangular plate with free edges. *Journal of Applied Mathematics and Mechanics*, 73(6):688–691, 2009.

[19] R. Courant and D. Hilbert. *Methods of Mathematical Physics*, volume 1. Springer, 1937.

[20] Sonelastic. Modulus of elasticity and poisson's coefficient of polymeric materials. https://www.sonelastic.com/en/fundamentals/tables-of-materials-properties/polymers.html.

[21] British Plastics Federation. Nylons (polyamide). https://www.bpf.co.uk/plastipedia/polymers/Polyamides.aspx.

[22] E. Crichton-Miller. Why violin makers' choice of wood is the key to perfection. *Financial Times*, 2022.

[23] North Carolina State University. Modal analysis of violin bodies with back plates made of different wood species. https://bioresources.cnr.ncsu.edu/resources/modal-analysis-of-violin-bodies-with-back-plates-made-of-different-wood-species/.

[24] D. W. Green, J. E. Winandy, and D. E. Kretschmann. *Wood Handbook - Wood as an engineering material.* Forest Products Laboratory, Forest Service, U. S. Dept. of Agriculture, 1999.

[25] P. W. Morse. *Vibration and Sound.* McGraw-Hill Book Company, Inc., 1948.

[26] C. Gough. Violin plate modes. *The Journal of the Acoustical Society of America*, 137, 2015.

[27] M. C. Pereyra and L. A. Ward. *Harmonic Analysis : From Fourier to Wavelets.* Student Mathematical Library, 2012.

Appendix A

Fourier series

In this section, some proofs will be given for theorems regarding Fourier series that were used in chapter 3. Section A.3 is taken from first year calculus notes by Paul Sutcliffe from the University of Durham [17].

A.1   The sine-cosine expansion

Theorem 3.3.1. Consider a function $f(x)$ of period 2L. The function can always be expressed in the form

$$f(x) = \frac{a_0}{2} + \sum_{n=1}^{\infty} \left(a_n \cos \left(\frac{n\pi x}{L} \right) + b_n \sin \left(\frac{n\pi x}{L} \right) \right) \tag{A.1}$$

where a_0, a_n, b_n are constants labelled by the positive integer n, and are called the Fourier coefficients of f(x). If these Fourier coefficients are such that this series converges then it is called the Fourier series of f(x).

Proof. The fact that the limit of the partial Fourier sums converges to the function $f(x)$ on $\mathbb{T} = [-L, L]$ (or $\mathbb{T} = [0, 2L]$ depending on our definition, but the proof may require re-paramterization) is not a trivial fact to prove, and in fact is not always true. To prove convergence everywhere on $\mathbb{T}$ requires us to impose additional constraints on f.

One such conditions is that if $f \in L^2(\mathbb{T})$, where $L^2(\mathbb{T})$ is the L^2 Lebesgue space on $\mathbb{T}$, then we can prove convergence almost everywhere (this is the same as saying that f must be square-integrable). To prove this also requires the concept of a "distance" between two functions, which is satisfied by imposing a metric on the space $L^2(\mathbb{T})$.

See reference [27] for a full proof of this. $\qquad \square$

A.2   The phase-amplitude expansion

Corollary 3.3.2. Consider a function f(x) of period 2L which is given on the interval $(-L, L)$. Then its Fourier series can alternatively be expressed in the form

$$f(x) = \frac{a_0}{2} + \sum_{n=1}^{\infty} \left(a_n \cos \left(\frac{n\pi x}{L} + \phi_n \right) \right) \tag{A.2}$$

for particular coefficients a_0, a_n.

Proof. We need to prove that the statements (A.1) and (A.2) are equivalent. We begin with statement (A.2). We can expand the cosine in (A.2) using trigonometric identities, to find that

$$f(x) = \frac{a_0}{2} + \sum_{n=1}^{\infty} \left(a_n \cos(\phi) \cos\left(\frac{n\pi x}{L}\right) - a_n \sin(\phi) \sin\left(\frac{n\pi x}{L}\right) \right). \tag{A.3}$$

This can be written as (A.1) by relabelling $a_n \cos(\phi) \longrightarrow a_n$, $-a_n \sin(\phi) \longrightarrow b_n$. $\qquad\square$

A.3   Calculating Fourier coefficients

Lemma 3.3.3. The Fourier coefficients a_n and b_n for periodic function with period 2L defined in the interval [0,2L] are given by

$$a_n = \frac{1}{L} \int_0^{2L} \cos\left(\frac{n\pi x}{L}\right) f(x) dx, \qquad b_n = \frac{1}{L} \int_0^{2L} \sin\left(\frac{n\pi x}{L}\right) f(x) dx. \tag{A.4}$$

Proof. We will begin by stating a few identities for the integrals of trigonometric functions.

$$\int_{-L}^{L} \cos\left(\frac{n\pi x}{L}\right) dx = 0. \tag{A.5}$$

$$\int_{-L}^{L} \sin\left(\frac{n\pi x}{L}\right) dx = 0. \tag{A.6}$$

$$\int_{-L}^{L} \sin\left(\frac{m\pi x}{L}\right) \cos\left(\frac{n\pi x}{L}\right) dx = 0. \tag{A.7}$$

$$\frac{1}{L} \int_{-L}^{L} \cos\left(\frac{m\pi x}{L}\right) \cos\left(\frac{n\pi x}{L}\right) dx = \delta_{mn}. \tag{A.8}$$

$$\frac{1}{L} \int_{-L}^{L} \sin\left(\frac{m\pi x}{L}\right) \sin\left(\frac{n\pi x}{L}\right) dx = \delta_{mn}. \tag{A.9}$$

The proofs of these identities are straightforward, and left for the reader. We then right the Fourier series of f(x) as

$$f(x) = \frac{a_0}{2} + \sum_{m=1}^{\infty} \left(a_m \cos\left(\frac{m\pi x}{L}\right) + b_m \sin\left(\frac{m\pi x}{L}\right) \right), \tag{A.10}$$

and then we can calculate

$$\frac{1}{L} \int_{-L}^{L} \cos\left(\frac{n\pi x}{L}\right) f(x) dx = \frac{1}{L} \int_{-L}^{L} \cos\left(\frac{n\pi x}{L}\right) \left[\frac{a_0}{2} + \sum_{m=1}^{\infty} \left(a_m \cos\left(\frac{m\pi x}{L}\right) + b_m \sin\left(\frac{m\pi x}{L}\right) \right) \right] dx$$

$$= \frac{a_0}{2L} \int_{-L}^{L} \cos\left(\frac{n\pi x}{L}\right) dx + \sum_{m=1}^{\infty} \left[\frac{a_m}{L} \int_{-L}^{L} \cos\left(\frac{n\pi x}{L}\right) \cos\left(\frac{m\pi x}{L}\right) dx + \frac{b_m}{L} \int_{-L}^{L} \cos\left(\frac{n\pi x}{L}\right) \sin\left(\frac{m\pi x}{L}\right) dx \right]$$

$$= \sum_{m=1}^{\infty} a_m \delta_{mn} = a_n. \tag{A.11}$$

Similarly

$$\frac{1}{L}\int_{-L}^{L}\sin\left(\frac{n\pi x}{L}\right)f(x)dx = \frac{1}{L}\int_{-L}^{L}\sin\left(\frac{n\pi x}{L}\right)\left[\frac{a_0}{2}+\sum_{m=1}^{\infty}\left(a_m\cos\left(\frac{m\pi x}{L}\right)+b_m\sin\left(\frac{m\pi x}{L}\right)\right)\right]dx$$

$$= \frac{a_0}{2L}\int_{-L}^{L}\sin\left(\frac{n\pi x}{L}\right)dx+\sum_{m=1}^{\infty}\left[\frac{a_m}{L}\int_{-L}^{L}\sin\left(\frac{n\pi x}{L}\right)\cos\left(\frac{m\pi x}{L}\right)dx+\frac{b_m}{L}\int_{-L}^{L}\sin\left(\frac{n\pi x}{L}\right)\sin\left(\frac{m\pi x}{L}\right)dx\right]$$

$$= \sum_{m=1}^{\infty}b_m\delta_{mn} = b_n. \tag{A.12}$$

To get the expression given in lemma 3.3.3, we can adjust the domain of the integrals due to the periodicity of f, and the trigonometric functions,

$$\frac{1}{L}\int_{-L}^{L}\sin\left(\frac{n\pi x}{L}\right)f(x)dx = \frac{1}{L}\int_{0}^{L}\sin\left(\frac{n\pi x}{L}\right)f(x)dx + \frac{1}{L}\int_{-L}^{0}\sin\left(\frac{n\pi x}{L}\right)f(x)dx$$

$$= \frac{1}{L}\int_{0}^{L}\sin\left(\frac{n\pi x}{L}\right)f(x)dx + \frac{1}{L}\int_{-L}^{0}\sin\left(\frac{n\pi(x+2L)}{L}\right)f(x+2L)dx$$

$$= \frac{1}{L}\int_{0}^{L}\sin\left(\frac{n\pi x}{L}\right)f(x)dx + \frac{1}{L}\int_{L}^{2L}\sin\left(\frac{n\pi u}{L}\right)f(u)du$$

$$= \frac{1}{L}\int_{0}^{2L}\sin\left(\frac{n\pi x}{L}\right)f(x)dx. \tag{A.13}$$

And likewise,

$$\frac{1}{L}\int_{-L}^{L}\cos\left(\frac{n\pi x}{L}\right)f(x)dx = \frac{1}{L}\int_{0}^{L}\cos\left(\frac{n\pi x}{L}\right)f(x)dx + \frac{1}{L}\int_{-L}^{0}\cos\left(\frac{n\pi x}{L}\right)f(x)dx$$

$$= \frac{1}{L}\int_{0}^{L}\cos\left(\frac{n\pi x}{L}\right)f(x)dx + \frac{1}{L}\int_{-L}^{0}\cos\left(\frac{n\pi(x+2L)}{L}\right)f(x+2L)dx$$

$$= \frac{1}{L}\int_{0}^{L}\cos\left(\frac{n\pi x}{L}\right)f(x)dx + \frac{1}{L}\int_{L}^{2L}\cos\left(\frac{n\pi u}{L}\right)f(u)du$$

$$= \frac{1}{L}\int_{0}^{2L}\cos\left(\frac{n\pi x}{L}\right)f(x)dx. \tag{A.14}$$

$\square$

Appendix B

Python code

B.1 Wave forms for the free square plate

B.1.1 Finding roots to the transcendental equations $\chi^{\pm}$

This code calculates an array of n values as solutions to either χ^+ or χ^- using the Newton-Raphson method. It was stored in the file "alphabetavalues.py".

```python
# Calculating the values of the numbers alpha and beta
# Where alpha = k * a and beta = q * b
# We are looking to solve chi_+-(g) = tan(g) +- tanh(g) = 0, where g = alpha or
    beta

import numpy as np
import scipy.optimize

def chi_plus(x):
    # Chi_plus = tan(x) + tanh(x)

    chi = np.tan(x) + np.tanh(x)
    return chi

def chi_minus(x):
    # Chi_plus = tan(x) - tanh(x)

    chi = np.tan(x) - np.tanh(x)
    return chi

def find_root(chi_function, i):

    return scipy.optimize.newton(func = chi_function, x0 = i)

def create_solutions_set_for_chi_plus(size):
    # Create an array of solutions for chi plus up to a given size

    i = 0
    values = []

    while len(values) < size:
        # Generate a new value of g that solves chi plus and add it to the array

        g = find_root(chi_plus, i)
        g = round(g, 4)
```

```python
        if g not in values:
            values.append(g)

        i = i+1.9

    return values

def create_solutions_set_for_chi_minus(size):
    # Create an array of solutions for chi minus up to a given size

    i = 0
    values = []

    while len(values) < size:
        # Generate a new value of g that solves chi minus and add it to the array

        g = find_root(chi_minus, i)
        g = round(g, 4)

        if g not in values:
            values.append(g)

        i = i+1.9

    return values

if __name__ == "__main__":

    # Calculate n values of g for chi plus () can be replaced with chi minus ()
    n = 5

    gs_chi_plus = create_solutions_set_for_chi_plus(n)

    print(gs_chi_plus)
```

B.1.2 Plotting the wave forms for the free square plate

This code produces a plot, heatmap, and Chladni pattern for the modes of vibration of the free rectangular plate. It was called "freeplates.py" and must be run from the same folder as "alphabetavalues.py".

```python
# Code to plot graphically the normal modes of vibration for a free square plate

import numpy as np
import matplotlib.pyplot as plt
import alphabetavalues



class Mode:

    def set_k(self, k):
        # Wavenumber k for the x component of the mode of vibration

        self.k = k
        return

    def set_q(self, q):
        # Wavenumber q for the y component of the mode of vibration

        self.q = q
        return

    def set_a(self, a):
        # The plate length in the x axis, -a <= x <= a

        self.a = a
        return

    def set_b(self, b):
        # The plate length in the x axis, -b <= x <= b

        self.b = b
        return

    def generateGrid(self, N):
        # Generate x-y grid for plotting the function

        self.N = N

        x = np.linspace(-self.a, self.a, N)
        y = np.linspace(-self.b, self.b, N)
        xs, ys = np.meshgrid(x, y, indexing='ij')

        self.x = x
        self.y = y
        self.xs = xs
        self.ys = ys
        return

    def cos_cos(self):
        # Generate the function that is symmetric in the x and y axes
```

```python
        k = self.k
        q = self.q
        a = self.a
        b = self.b

        xs = self.xs
        ys = self.ys

        zs = np.cos(k*xs)*np.cos(q*ys) - \
            ((np.sin(k*a)*np.sin(q*b))/(np.sinh(k*a)*np.sinh(q*b)))*np.cosh(k*xs)*np.cosh(q*ys)

        zs = zs*0.25

        self.zs = zs

    def sin_cos(self):
        # Generate the function that is symmetric about the x axis

        k = self.k
        q = self.q
        a = self.a
        b = self.b

        xs = self.xs
        ys = self.ys

        zs = np.sin(k*xs)*np.cos(q*ys) + \
            ((np.cos(k*a)*np.sin(q*b))/(np.cosh(k*a)*np.sinh(q*b)))*np.sinh(k*xs)*np.cosh(q*ys)

        zs = zs*0.25

        self.zs = zs

    def cos_sin(self):
        # Generate the function that is symmetric about the y axis

        k = self.k
        q = self.q
        a = self.a
        b = self.b

        xs = self.xs
        ys = self.ys

        zs = np.cos(k*xs)*np.sin(q*ys) + \
            ((np.sin(k*a)*np.cos(q*b))/(np.sinh(k*a)*np.cosh(q*b)))*np.cosh(k*xs)*np.sinh(q*ys)

        zs = zs*0.25

        self.zs = zs

    def sin_sin(self):
        # Generate the function that is anti-symmetric in the x and y axes

        k = self.k
        q = self.q
        a = self.a
        b = self.b
```

```python
        xs = self.xs
        ys = self.ys

        zs = np.sin(k*xs)*np.sin(q*ys) -
            ((np.cos(k*a)*np.cos(q*b))/(np.cosh(k*a)*np.cosh(q*b)))*np.sinh(k*xs)*np.sinh(q*ys)

        zs = zs*0.25

        self.zs = zs

def plotMode(mode):
    # Plot the function
    fig = plt.figure(figsize = (12,10))
    ax = plt.axes(projection='3d')
    ax.grid()


    surf = ax.plot_trisurf(mode.xs.flatten(), mode.ys.flatten(),
        mode.zs.flatten(), edgecolor="black", linewidth=0.1, antialiased=True,
        cmap = 'inferno')

    # Set axes label
    ax.set_xlabel('x', labelpad=20)
    ax.set_ylabel('y', labelpad=20)
    ax.set_zlabel('z', labelpad=20)

    # Set colorbar
    fig.colorbar(surf, shrink=0.5, aspect=8)

    plt.show()




def plotHeatMap(mode):
    # Heatmap

    arr = np.rot90(mode.zs, 3)
    m = np.flip(arr, 1)


    plt.imshow(m, cmap='inferno', origin="lower")
    plt.colorbar()

    plt.show()




def plotChladniPattern(mode):
    # Generating and plotting the Chaldni patterns

    fig = plt.figure(figsize=(6,6))

    # Find all points of low amplitude
    indcs = np.where(abs(mode.zs) < 0.05)

    # zip the 2 arrays to get the exact coordinates
    listOfCoordinates= list(zip(indcs[0], indcs[1]))
```

```python
    # Store the x values of each point where the amplitude is small
    chld_x = []
    # Store the y values of each point where the amplitude is small
    chld_y = []

    for cord in listOfCoordinates:
        chld_x.append(mode.xs[cord])
        chld_y.append(mode.ys[cord])

    plt.scatter(chld_x, chld_y, color="orangered")
    plt.show()



if __name__ == "__main__":
    # Plot the graph

    # How many values of alpha or beta we need to plot the mode
    s = 11

    gamma_plus = alphabetavalues.create_solutions_set_for_chi_plus(s)
    gamma_minus = alphabetavalues.create_solutions_set_for_chi_minus(s)

    # Generate an instance of the mode
    mode = Mode()

    # Define size of plate: -a < x < a , -b < y < b
    a = 1
    b = 1
    k = (gamma_minus[1])/a
    q = (gamma_minus[1])/b


    # Set parameters
    mode.set_k(k)
    mode.set_q(q)
    mode.set_a(a)
    mode.set_b(b)

    # Set gridsize, N
    N = 50

    # Calculate the values of the function
    mode.generateGrid(N)
    mode.sin_sin()

    plotMode(mode)

    plotHeatMap(mode)

    plotChladniPattern(mode)
```

B.2 Numerical solutions to the Kirchoff-Love equation for the violin

B.2.1 4ᵗʰ order Runge-Kutta integration of ODEs

The following code was written by my supervisor Professor Bernard Piette and is used to perform 4ᵗʰ order Runge-Kutta integration of an ordinary differential equation. The file is named "ode_rk4.py". This code was not written by the author but has been included because it is required for the code in section B.2 to run.

```python
import matplotlib.pyplot as plt
import numpy as np

class ODE_RK4:
  """ A class to compute the time evolution of a population using the
      fourth order Runge-Kutta method.
  """

  def __init__(self, V0=[0], dt=0.1, t0=0):
      """ Set the variables used by the class:

      :param V0 : initial value (as an array or a list)
      :param dt : integration time step
      :param t0 : initial time
      """
      self.reset(V0, dt=dt, t0=t0)

  def reset(self, V0, dt, t0=0):
      """ Reset the integration parameters; see __init__ for more info."""

      self.V = np.array(V0, dtype='float64') # ensure we use floats!
      self.dt = dt
      self.t = t0
      self.t_list = [] # to store t values for plots
      self.V_list = [] # to store f values for plots

  def F(self, t, V):
      """ Return the right hand side of the equation dV/dt = F(t,V)."""
      pass

  def one_step(self):
      """ Perform a single integration step of the 4th order Runge Kutta
          method."""

      k1 = self.F(self.t, self.V)
      K = self.V+0.5*self.dt*k1
      self.boundary(K)

      k2 = self.F(self.t+0.5*self.dt, K)
      K = self.V+0.5*self.dt*k2
      self.boundary(K)

      k3 = self.F(self.t+0.5*self.dt, K)
      K = self.V+self.dt*k3
      self.boundary(K)

      k4 = self.F(self.t+self.dt, K)
      # self.v -> v(t+dt)
```

```python
        self.V += self.dt/6.0*(k1+2.0*(k2+k3)+k4)
        self.boundary(self.V)

        # t -> t + dt
        self.t += self.dt

    def boundary(self, v):
        pass

    def iterate(self, tmax, fig_dt=-1):
        """ Solve the system of equations DN/dt = F(N) until t=tmax.
            Save N and t in lists N_list and t_list every fig_dt.

        :param tmax  : integration upper bound
        :param fig_dt : interval between data point for figures (use dt if < 0)
        """

        if(fig_dt < 0) : fig_dt = self.dt*0.99 # same all data

        next_fig_t = self.t*(1-1e-15) # ensure we save the initial values

        tmax -= self.dt*1e-12 # stop as close to tmax as possible
        while(self.t < tmax): # integrate until tmax
          self.one_step()
          if(self.t >= next_fig_t): # save fig when next_fig_t is reached
            self.V_list.append(np.array(self.V)) # force a copy of V!
            self.t_list.append(self.t)
            next_fig_t += fig_dt # set the next figure time

    def plot(self, i, j=0, style="k-"):
        """ plot V[i] versus t  (i > 1 and j = 0) using format
            plot V[i] versus V[j] (i > 1 and j > 1) using format
            plot t   versus V[j] (i = 0 and j > 1) using format

        :param i : index of function for abscissa
        :param j : index of function for ordinate
        :param format : format for the plot function
        """

        if(j==0):
          lx = self.t_list
        else: # extra item i-1 from each element of f_list
          lx = list(map (lambda v : v[j-1] , self.V_list))
        if(i==0):
          ly = self.t_list
        else:
          ly = list(map (lambda v : v[i-1] , self.V_list))
        plt.plot(lx, ly, style);


# Tests for this module; only run when not importing the module.

if __name__ == "__main__":
  class RK4Test(ODE_RK4):
    def F(self, t, V):
        """ Sample of two ODEs: du/dt = v; dv/dt = -u. """
        return(np.array([self.V[1], -self.V[0]]))
```

```python
pop = RK4Test(V0=[1.0, 0.0], dt=0.001)
pop.iterate(10, 0.1)
pop.plot(1,0, "r-")
pop.plot(2,0, "b-")
plt.show()
pop.plot(1,2, "g-")
plt.axis('equal')
plt.margins(0.1, 0.1)
plt.show()
```

B.2.2   2-dimensional PDE integration on the violin-shaped plate

The following code was produced by the author as a modification of code written by
supervisor Professor Bernard Piette in order to performs Runge-Kutta integration of a
2-dimensional partial differential equation by decomposing it into ODEs. The partial differential equation used in this code is the Kirchoff-Love equation with driving and damping
forces (equation 5.14) and the fixed edge boundary condition is imposed on the hippopede
shape shown in figure 5.1. The code was named "my_PDE2d_Base.py" and must be run
from the same directory as "ode_rk4.py".

```python
import sys
import ode_rk4
import numpy as np
import matplotlib.pyplot as plt

class PDE_Base(ode_rk4.ODE_RK4):
  """ A class to solve partial differential equations by
      rewriting them as a system of ordinary differential
      equations.
  """

  def __init__(self, k, Lx, Nx, Ny):
      """Initialiser for our class.
         L : total plate width - I don't think these are needed?
         N : number of nodes
         k : constant in equation
      """
      self.k = k # equation parameter
      self.Nx = Nx # number of points
      self.Ny = Ny # number of points
      self.Lx = Lx
      self.dx = Lx/(Nx-1)
      self.dy = self.dx # for accuracy: keep dy = dx
      self.Ly = self.dy *Ny
      self.dt = (self.dx**2)/(np.sqrt(self.k)*4)
      # we use an empty array for now
      super().reset(np.empty([self.Nx,self.Ny,2], dtype='float64'),\
                    self.dt, t0=0)


  def reset(self, t, v0, dv0):
      """ Initialise the paramaters (t and initial conditions)
         v0 : initial configuration
         dv0 : initial time derivative
      """
      self.t = t

      if v0.shape != (self.Nx,self.Ny) or dv0.shape != (self.Nx,self.Ny):
        print("PDE_Base.__init__ ERROR: invalid size for v0 or dv0")
        sys.exit(5)

      # Create array to hold the functions y and dy/dt
      V = np.empty([self.Nx,self.Ny,2], dtype='float64')
      # v[0:N]  : y
      # v[N:2*N] : dy/dt
      V[:,:,0] = v0 # v
      V[:,:,1] = dv0 # dv
```

```python
        super().reset(V, self.dt, t0=t)

    def F(self,t,v):
        """ equation to solve:
            d dv[i]/dt = -k*( (v[i+2,j] - 4v[i+1,j] + 6v[i,j] - 4v[i-1,j] +
                v[i-2,j])
                        2*(v[i+1,j]+ v[i-1,j]-2*v[i,j])*(v[i,j+1]+
                            v[i,j-1]-2*v[i,j]) +
                        (v[i,j+2] - 4v[i,j+1] + 6v[i,j] - 4v[i.j-1] + v[i,j-2]) )
            t: current time
            v: current function as a vector
        """
        eq = np.zeros([self.Nx,self.Ny,2])

        dvdxx = (v[2:,1:-1,0]+v[0:-2,1:-1,0]-2*v[1:-1,1:-1,0])/self.dx**2
        dvdyy = (v[1:-1,2:,0]+v[1:-1,0:-2,0]-2*v[1:-1,1:-1,0])/self.dy**2
        dvdxxxx =
            (v[4:,2:-2,0]-4*v[3:-1,2:-2,0]+6*v[2:-2,2:-2,0]-4*v[1:-3,2:-2,0]+v[0:-4,2:-2,0])/self.dx*
        dvdyyyy =
            (v[2:-2,4:,0]-4*v[2:-2,3:-1,0]+6*v[2:-2,2:-2,0]-4*v[2:-2,1:-3,0]+v[2:-2,0:-4:,0])/self.dy

        # Ignore the first and last row and column from the matrices dvdxx and
            dvdyy
        dvdxx = dvdxx[1:-1,1:-1]
        dvdyy = dvdyy[1:-1,1:-1]

        # d doty[i]/dt = k*dx^2(y[i+1]+y[i-1]-2y[i])
        eq[2:-2,2:-2,0] = v[2:-2,2:-2,1] # d v/dt = dv

        # Damping parameter
        gamma = 1

        # The Kirchoff-Love equation
        # d dv/dt = k (dd v/dxx+ dd v/dyy) - gamma * dv
        eq[2:-2,2:-2,1] = -self.k*(dvdxxxx + 2*np.multiply(dvdxx,dvdyy) + dvdyyyy)
            + gamma*eq[2:-2,2:-2,0]


        # specify coordinate of driving point
        g = 0.1 # force amplitude
        f= 1000.0# frequency of driving
        eq[self.Nx//2,self.Ny//2,1] -= (1*10**(-3) *
            (2*np.pi*f)**2)*np.sin(2*np.pi*f*t)


        return(eq)

    def boundary(self, v):
        # set all edges to zero.

        # For the 100 by 100 square
        # Imposes the boundary condition as a violin-shape on that v=0 and dv=0 on
            the edge of, and outside, the plate
        for x in range (0,self.Nx):
            for y in range (0,self.Ny):

                # The coefficient c for c x^2 must be equal to the square of the
```

```
                    maximinum value of x in the square, with (0,0) at the center.
            # This means that c = (Nx/2)^2
            # The coefficient d is then calculated by the ratio d = 3/25 times c

            if (((x-self.Nx/2)**2 + (y-self.Ny/2)**2)**2 >=
                ((self.Nx/2)**2)*(x-self.Nx/2)**2 +
                (3/25)*((self.Nx/2)**2)*(y-self.Ny/2)**2) and (x != self.Nx/2
                and y != self.Ny/2): #hippopede filling up the square
                v[x,y,:] = 0.0
            elif abs(y) >= np.sqrt((3/25)*((self.Nx/2)**2)) and x == self.Nx/2:
                v[x,y,:] = 0.0
            else:
                pass

    def plot_snapshots(self, fig_dt, fname=""):
        """ Plot profile snapshot at various intervals during the first half
            of the period.
            Ns: number of snapshots to display
            T: period of oscillation
            fig_dt: time intervals between saved configurations
            fname: filename for figure outout
        """
        # x coordinate values
        # T/fig_dt : number of sample within 1 period
        # take Ns profile during the first half of the period
        t = 0;
        next_t = 0
        i = 0
        while(i < len(self.t_list)):
          if t >= next_t:
            plt.close("all")
            next_t == fig_dt
            fig_name = fname+"_"+str(i)+".png"
            plt.imshow(self.V_list[i][:,:,0],cmap='hot')
            plt.colorbar()
            i += 1
            if fname=="":
              plt.show()
            else:
              plt.savefig(fig_name)
          t = t+self.dt


#########################################################

if __name__ == "__main__":

  # model PARAMETERS
  # k = 1 - outdated

  # Calculate k
  # In our equation...
  # We get k = 18

  k = 18.0


  L = 0.36
```

```python
N = 100 # Nx=Ny
tmax = 1.0 # integration duration
fig_dt = 0.1 # interval between figures
# Needed to initialise dx
my_pde = PDE_Base(k, L, N, N)

# Initial condition
x = np.linspace(-L/2,L/2,N)
y = np.linspace(-L/2,L/2,N)
xv,yv = np.meshgrid(x,y)

dv0 = np.zeros([N,N],dtype='float64')

v0 = np.zeros([N,N],dtype='float64')

my_pde.reset(0, v0, dv0)
my_pde.iterate(tmax, fig_dt=1)
my_pde.plot_snapshots(fig_dt, fname="violin_test") # fname non empty ->
                                    # generate pdf file for each graph
print("Finished")
```